

# STUDY OF THE TENSOR FORCE CONTRIBUTION IN THE OXYGEN ISOTOPES USING QFS REACTIONS

Barrière Antoine, Mozumdar Nikhil, Sorlin Olivier  
and the R3B Collaboration



UNIVERSITÉ  
CAEN  
NORMANDIE



# Study of the evolution of proton $p_{3/2} - p_{1/2}$ SO splitting between $^{16}\text{O}$ and $^{22}\text{O}$

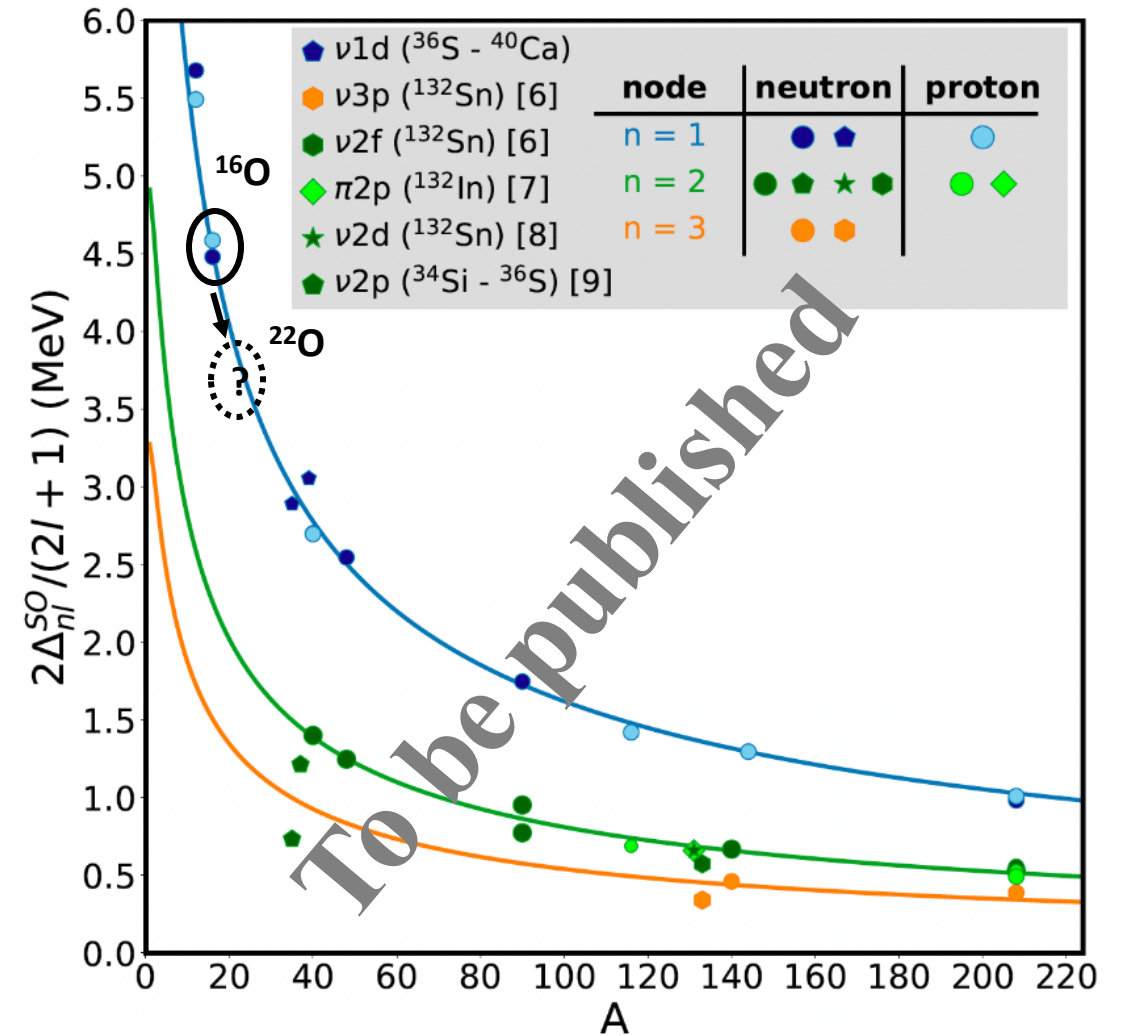
In the shell model framework, the nuclear interaction can be divided in several parts:

- Central
- Spin-orbit
- Tensor

A review[1] and global fit based mostly on stable nuclei data reproduces the SO splitting with the following function :

$$\Delta_{SO} = \frac{24.5}{n} (l + 1/2) A^{-0.597}$$

The factor  $\sim A^{-2/3}$  is the fingerprint of the role of the SO interaction in this trend (surface term).



Trend of Mairle[1] and review of new physics cases

[1] G. Mairle, Phys. Lett. B **304** (1993) 39.

[2] S. Jongile *et al.* to be submitted to Nature Physics.

# Study of the evolution of proton $p_{3/2} - p_{1/2}$ SO splitting between $^{16}\text{O}$ and $^{22}\text{O}$

In the shell model framework, the nuclear interaction can be divided in several parts:

- Central
- Spin-orbit
- Tensor

A review[1] and global fit based mostly on stable nuclei data reproduces the SO splitting with the following function :

$$\Delta_{SO} = \frac{24.5}{n} (l + 1/2) A^{-0.597}$$

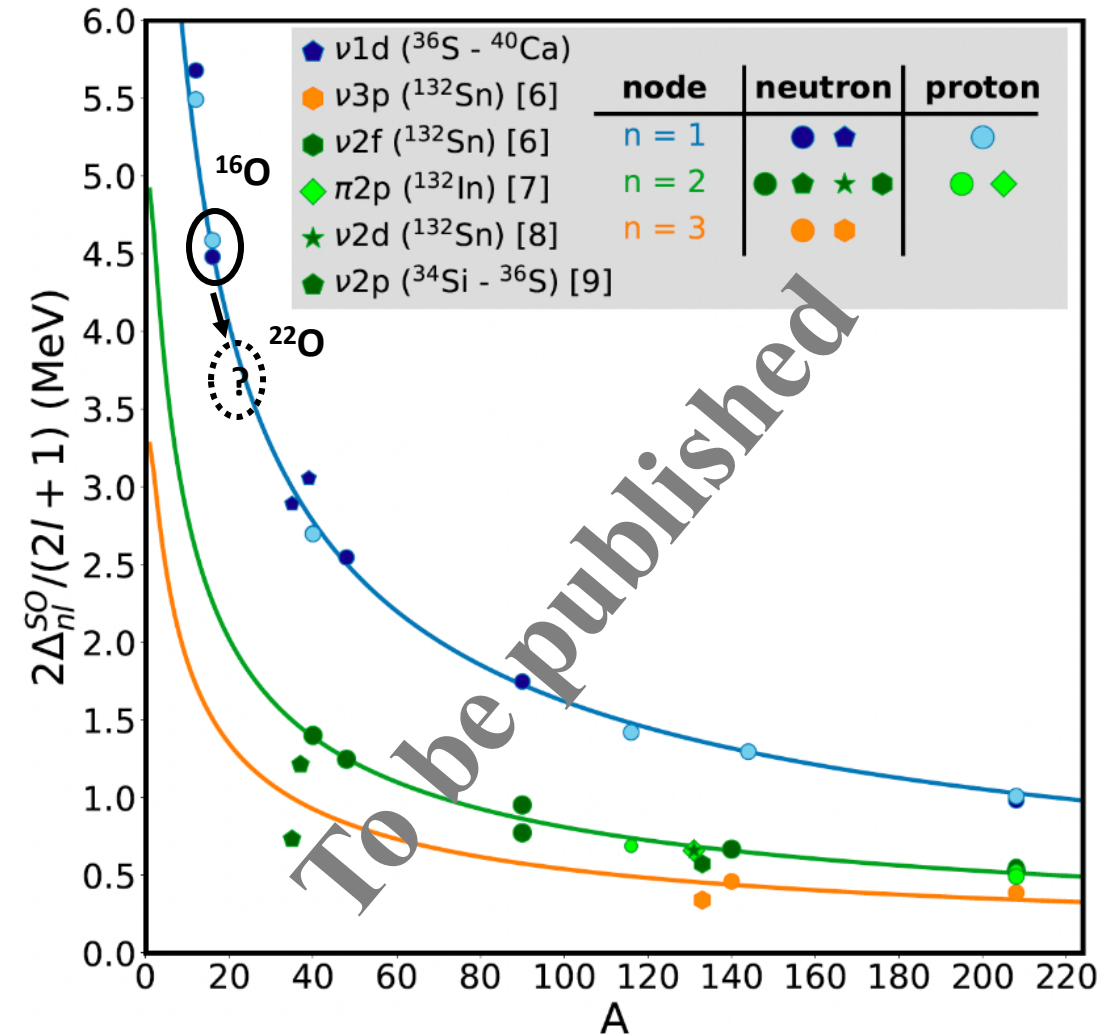
The factor  $\sim A^{-2/3}$  is the fingerprint of the role of the SO interaction in this trend (surface term).

Estimation of the proton gap  $0p_{1/2} - 0p_{3/2}$  :

in  $^{16}\text{O}$  --> 7.02 MeV

in  $^{22}\text{O}$  --> 5.81 MeV

**Deviations from this trend may be due to the tensor force contribution**



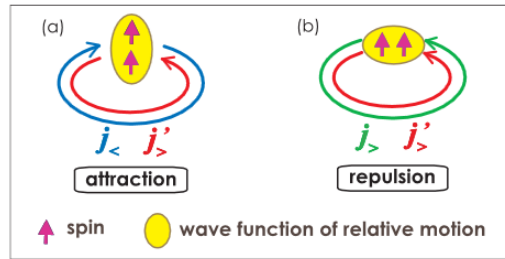
Trend of Mairle[1] and review of new physics cases

[1] G. Mairle, Phys. Lett. B **304** (1993) 39.

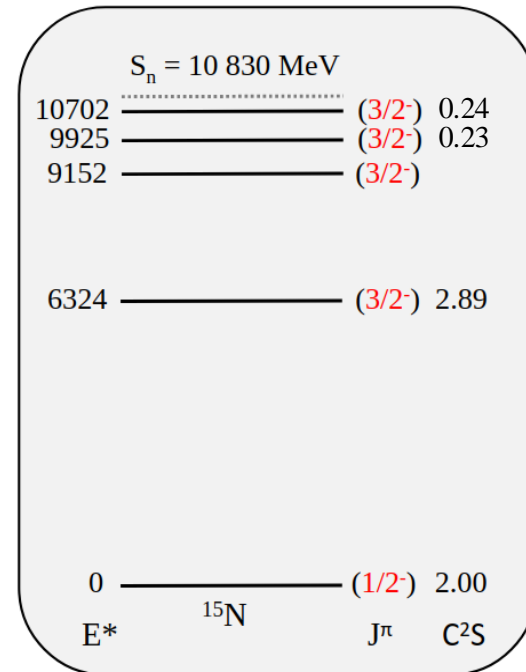
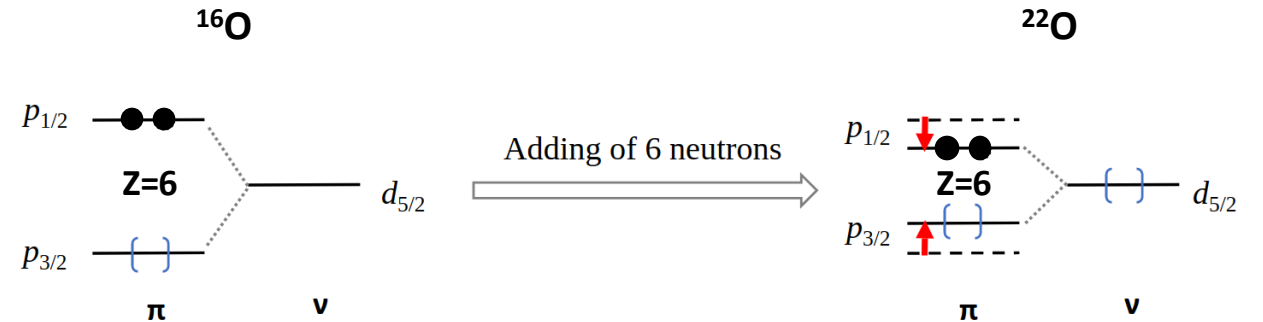
[2] S. Jongile *et al.* to be submitted to Nature Physics.

# Role of tensor force in the O isotopic chain

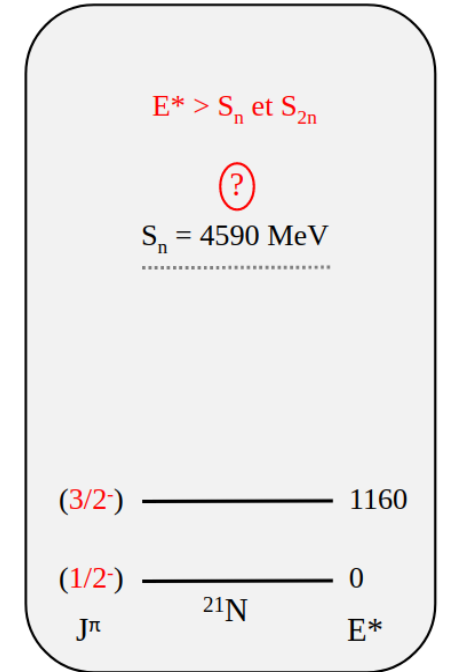
Tensor interaction [3]:



The tensor force should then reduce the spin-orbit splitting  $0p_{1/2} - 0p_{3/2}$  (proton) in the O isotopic chain, when the  $0d_{5/2}$  (neutron) is filled.



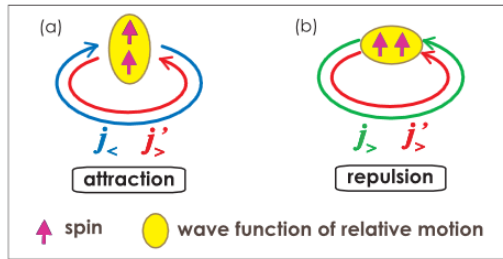
6 neutrons in  
the  $d_{5/2}$  orbital



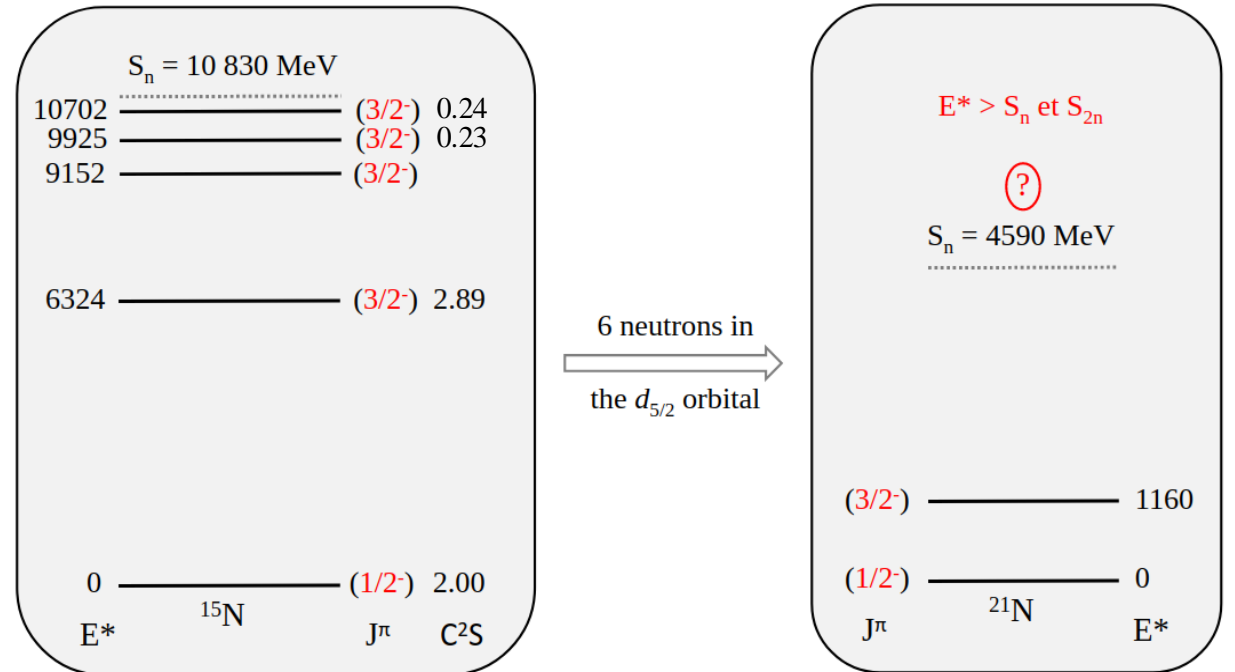
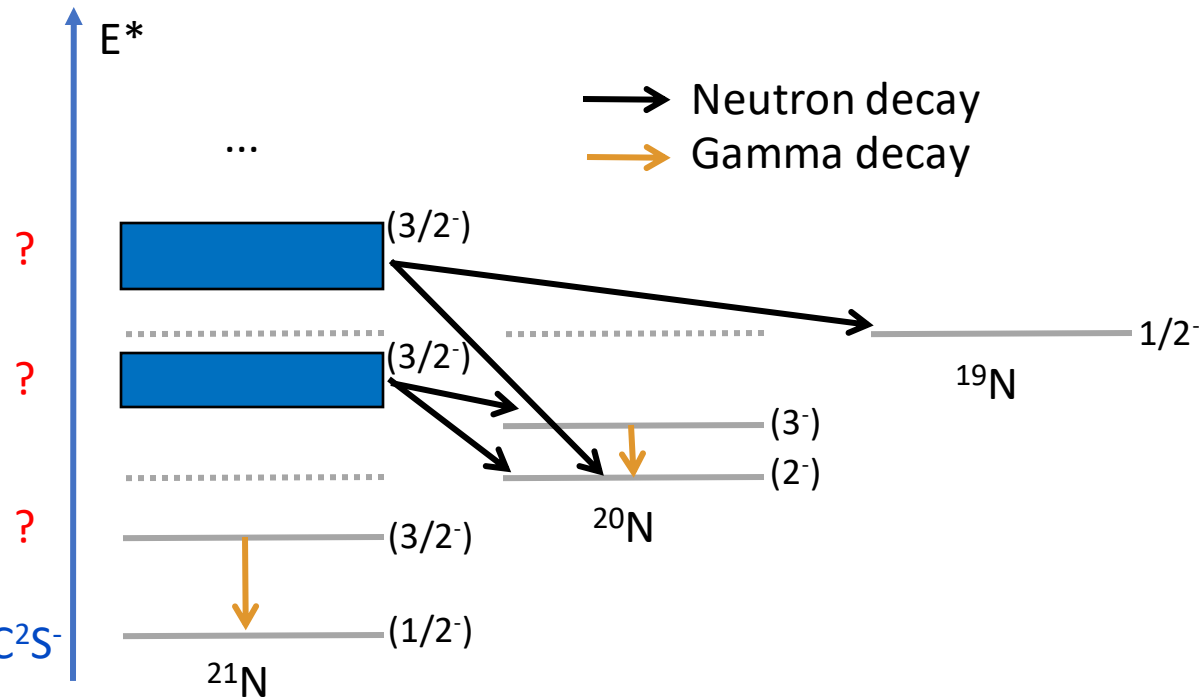
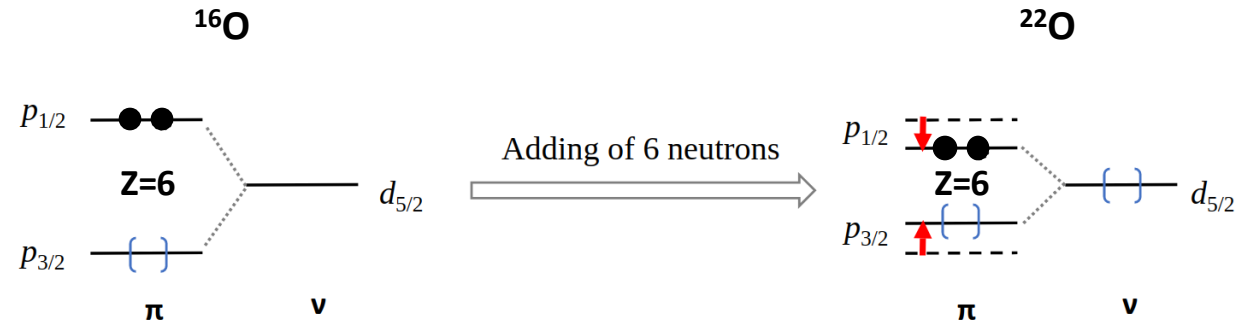
[3] T.Otsuka *et al*, PRL **95** (2005) 232502.

# Role of tensor force in the O isotopic chain

Tensor interaction [3]:



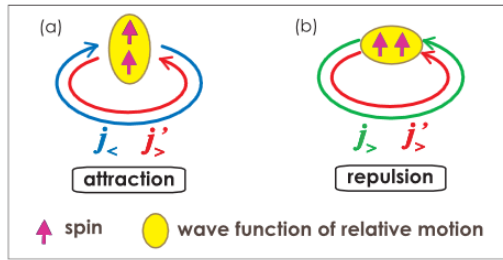
The tensor force should then reduce the spin-orbit splitting  $0p_{1/2} - 0p_{3/2}$  (proton) in the O isotopic chain, when the  $0d_{5/2}$  (neutron) is filled.



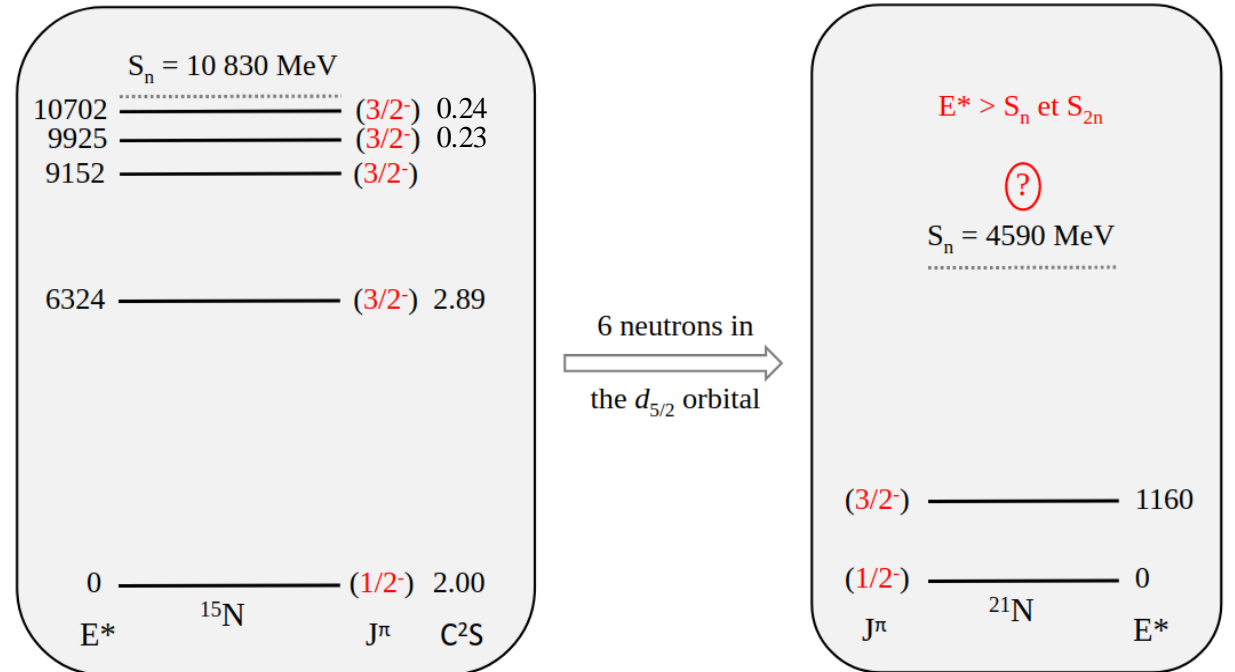
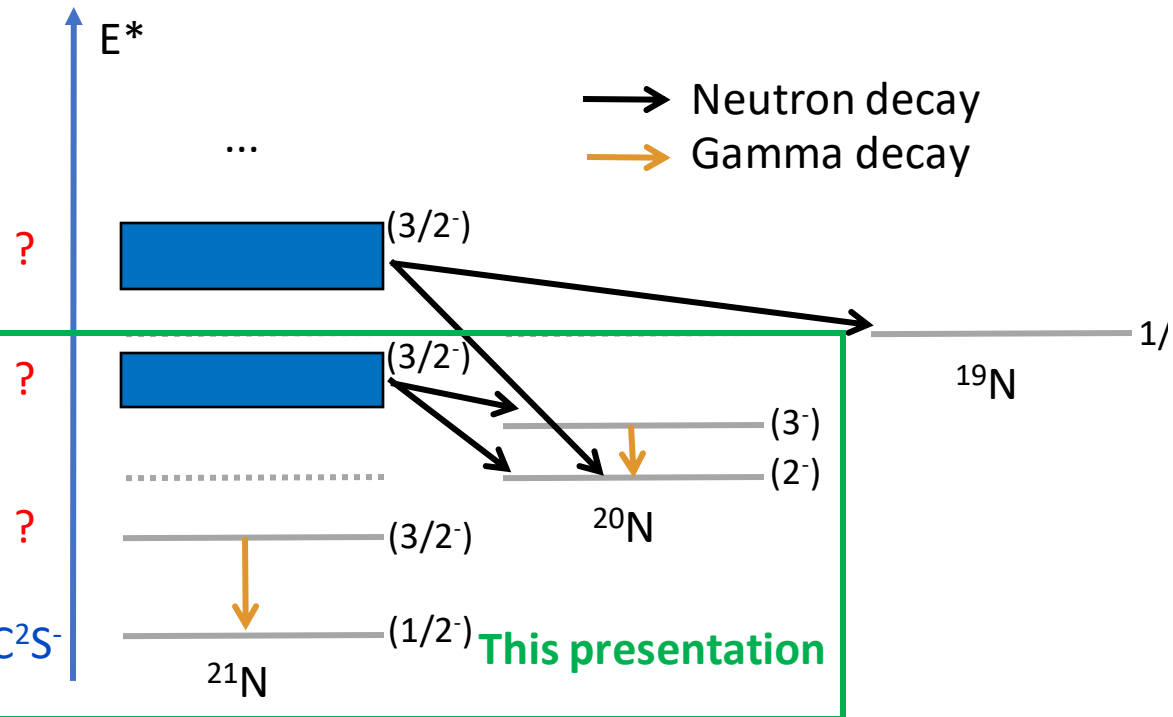
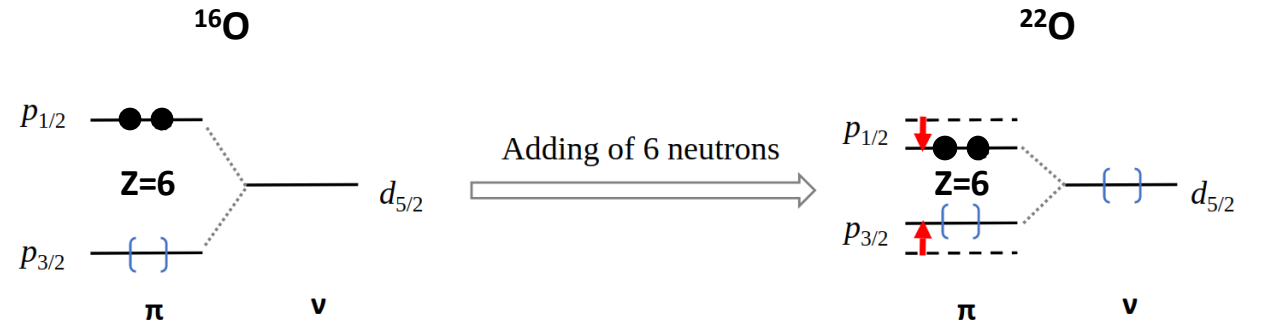
[3] T.Otsuka *et al*, PRL **95** (2005) 232502.

# Role of tensor force in the O isotopic chain

Tensor interaction [3]:



The tensor force should then reduce the spin-orbit splitting  $0p_{1/2} - 0p_{3/2}$  (proton) in the O isotopic chain, when the  $0d_{5/2}$  (neutron) is filled.



[3] T.Otsuka *et al*, PRL **95** (2005) 232502.

# Experimental setup

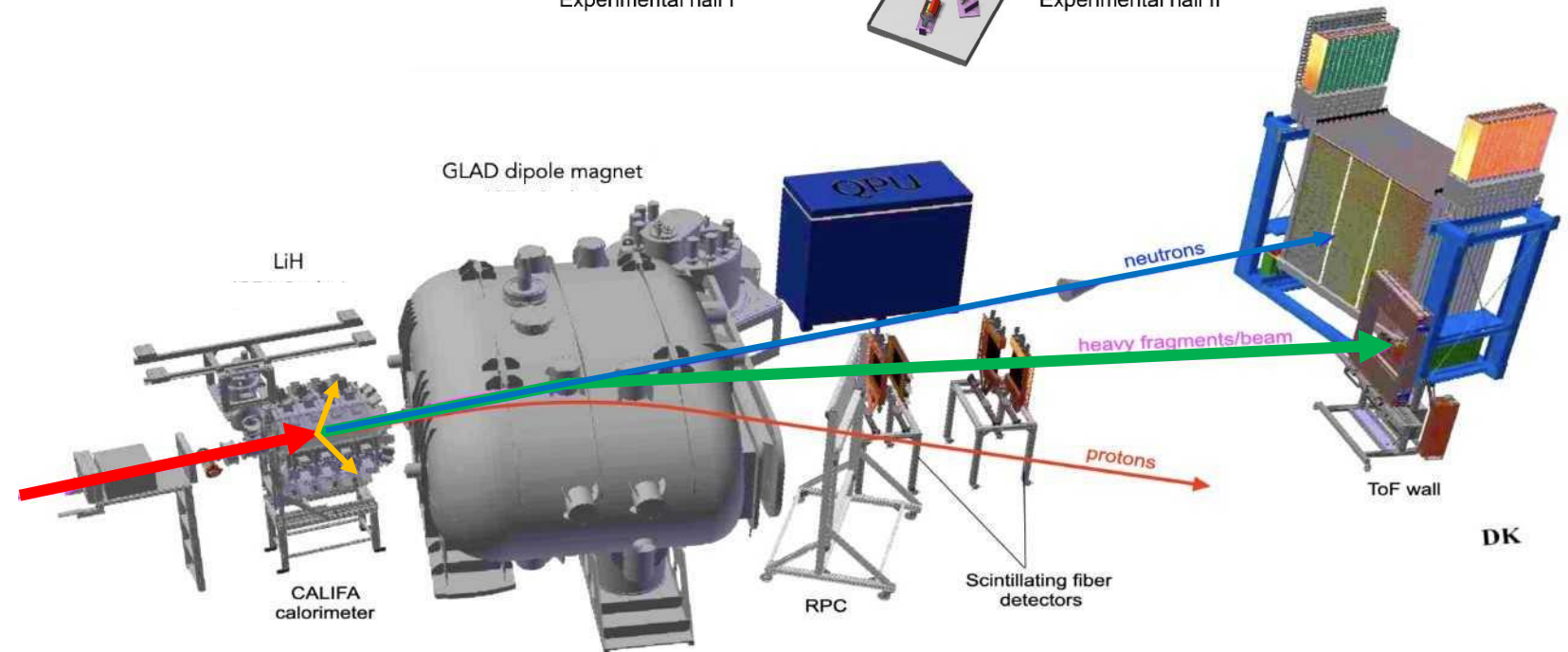
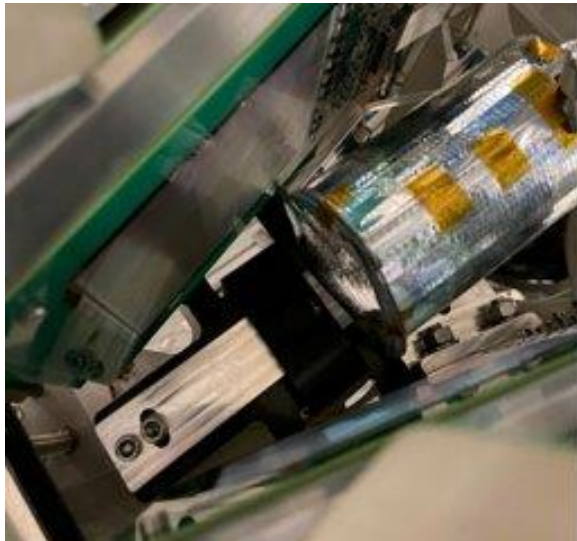
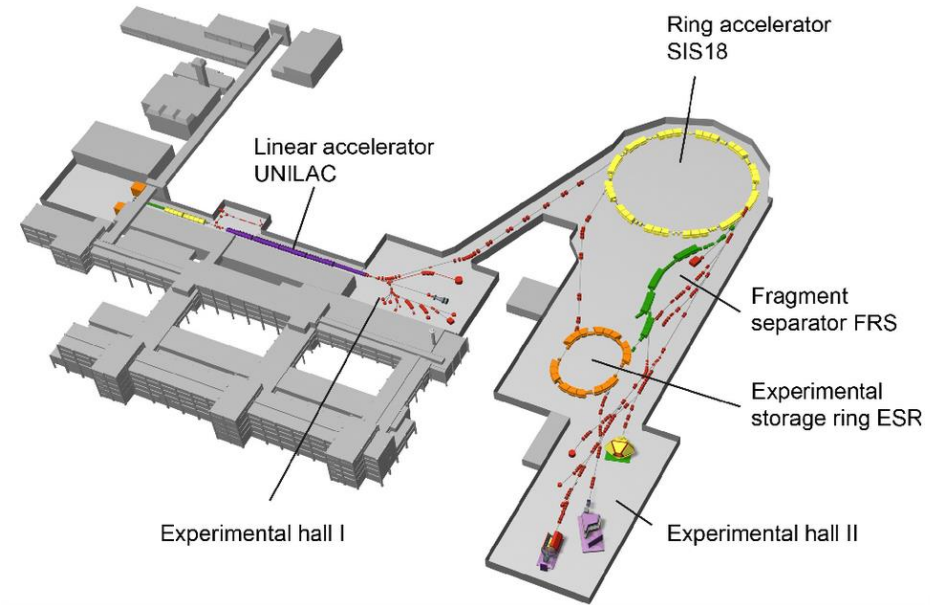
R<sup>3</sup>B setup at GSI

Cocktail beam from FRS (2 beam settings)

Beam energy: ~550MeV/A

QFS reaction e.g.  $(p,pn)$  and  $(p,2p)$  in LiH

Complete measurement in inverse kinematics:



# Experimental setup

R<sup>3</sup>B setup at GSI

Cocktail beam from FRS (2 beam settings)

Beam energy: ~550MeV/A

QFS reaction e.g.  $(p,pn)$  and  $(p,2p)$  in LiH

Complete measurement in inverse kinematics:

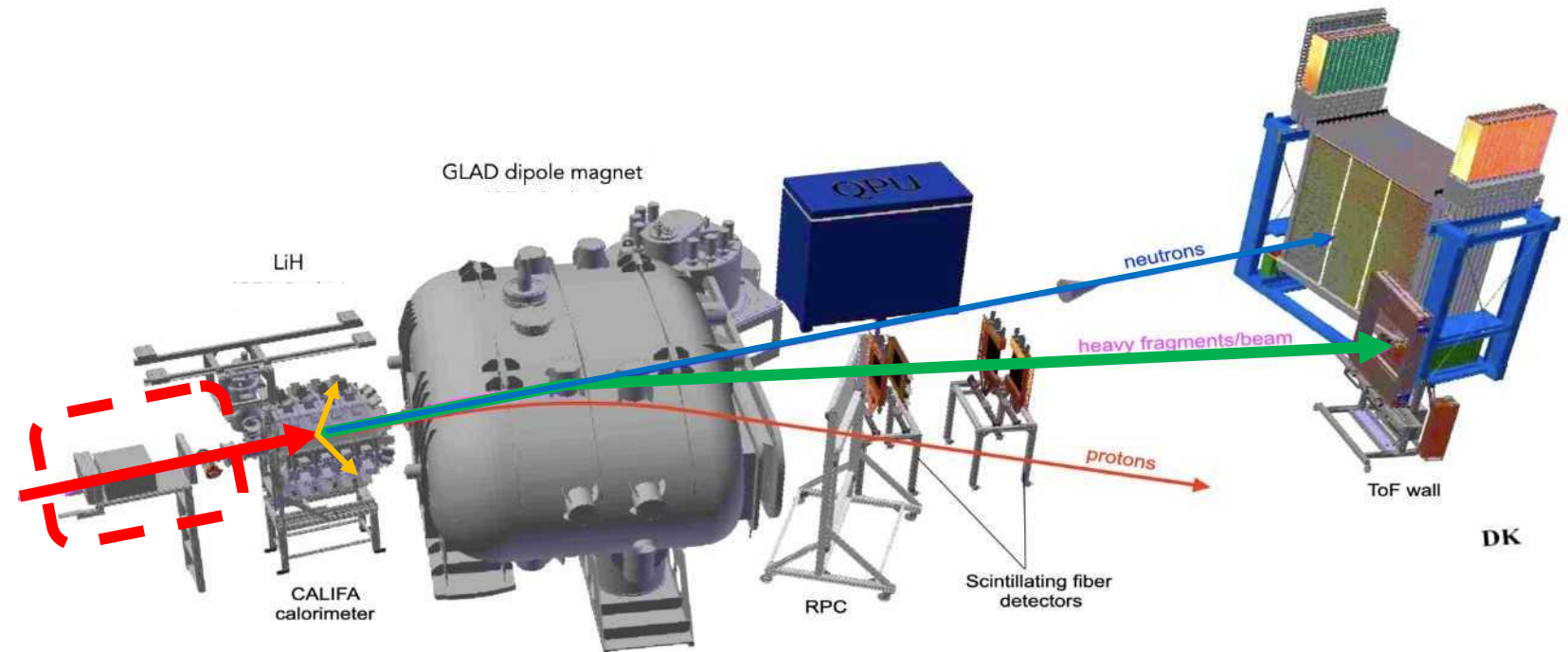
- **Incoming nucleus;**



LOS (t)



MusLi ( $\Delta E$ ) + MWPC (x,y)





# Experimental setup

R<sup>3</sup>B setup at GSI

Cocktail beam from FRS (2 beam settings)

Beam energy: ~550MeV/A

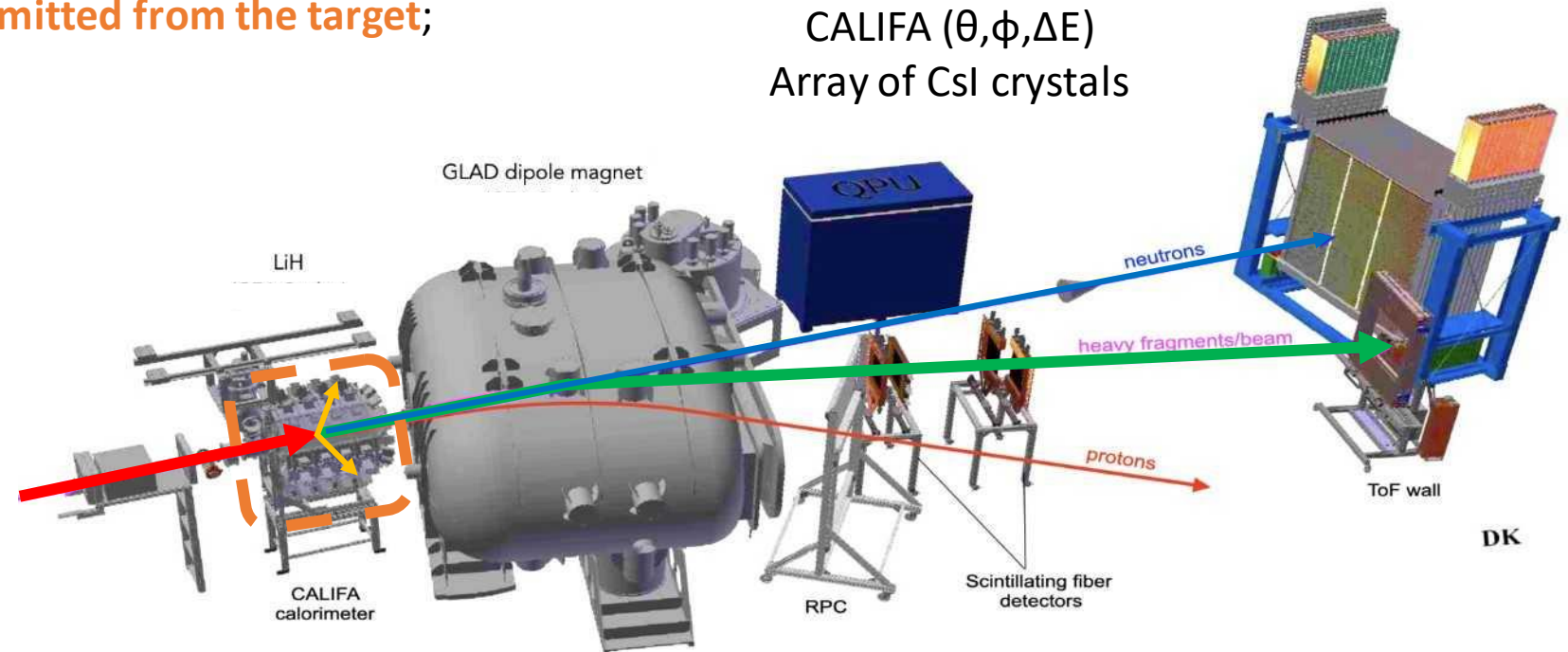
QFS reaction e.g.  $(p,pn)$  and  $(p,2p)$  in LiH

Complete measurement in inverse kinematics:

- **Incoming nucleus;**
- **Light particles and gammas emitted from the target;**



CALIFA ( $\theta, \phi, \Delta E$ )  
Array of CsI crystals



# Experimental setup

R<sup>3</sup>B setup at GSI

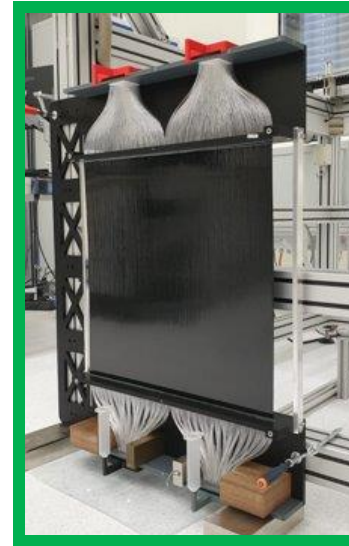
Cocktail beam from FRS (2 beam settings)

Beam energy: ~550MeV/A

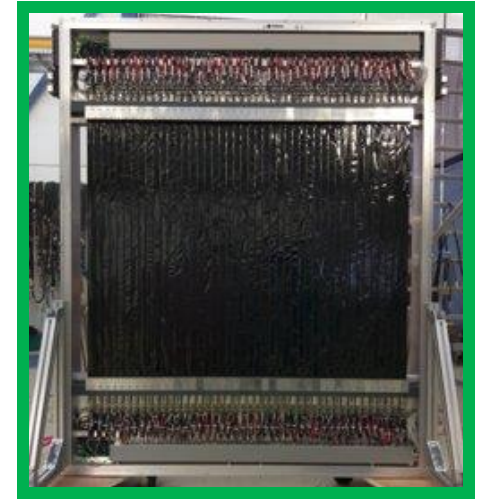
QFS reaction e.g.  $(p,pn)$  and  $(p,2p)$  in LiH

Complete measurement in inverse kinematics:

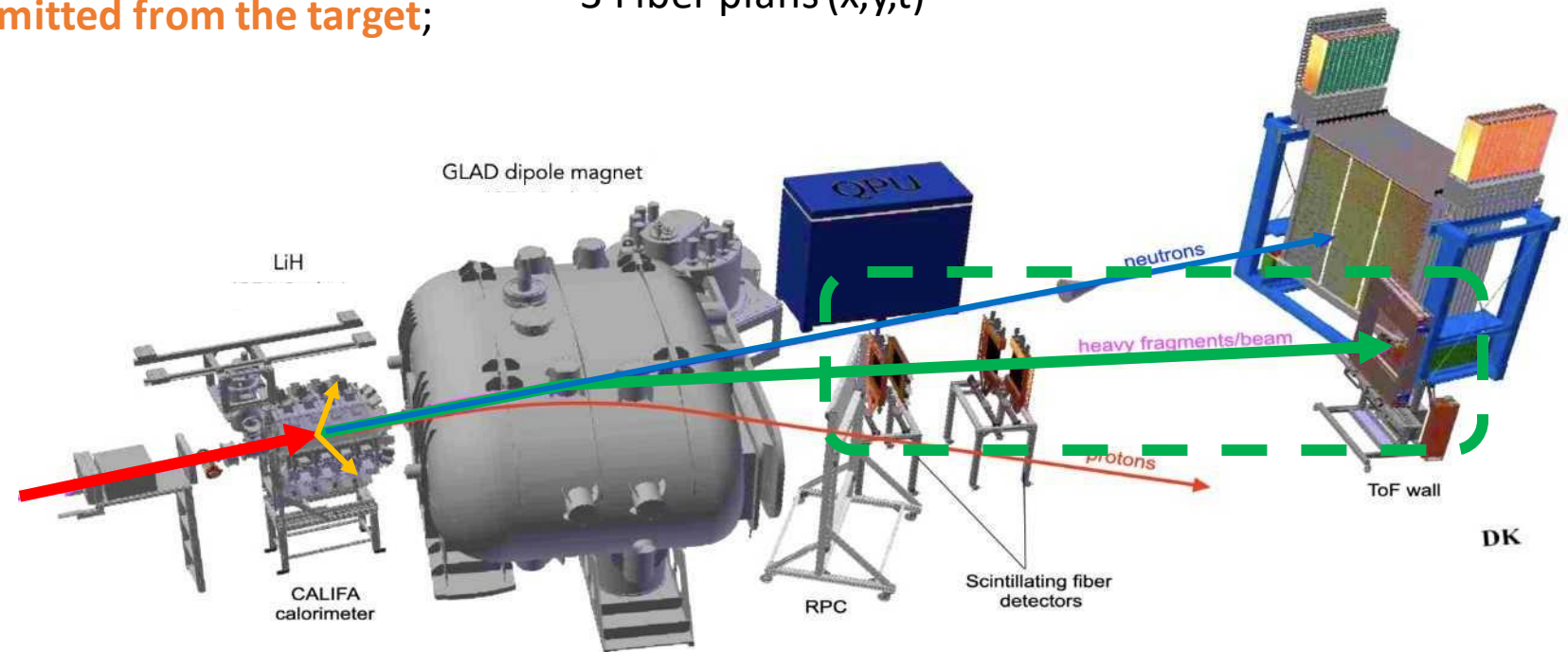
- **Incoming nucleus;**
- **Light particles and gammas emitted from the target;**
- **Outgoing fragment;**



3 Fiber plans (x,y,t)



ToFD (x,y,t,ΔE)



# Experimental setup

R<sup>3</sup>B setup at GSI

Cocktail beam from FRS (2 beam settings)

Beam energy: ~550MeV/A

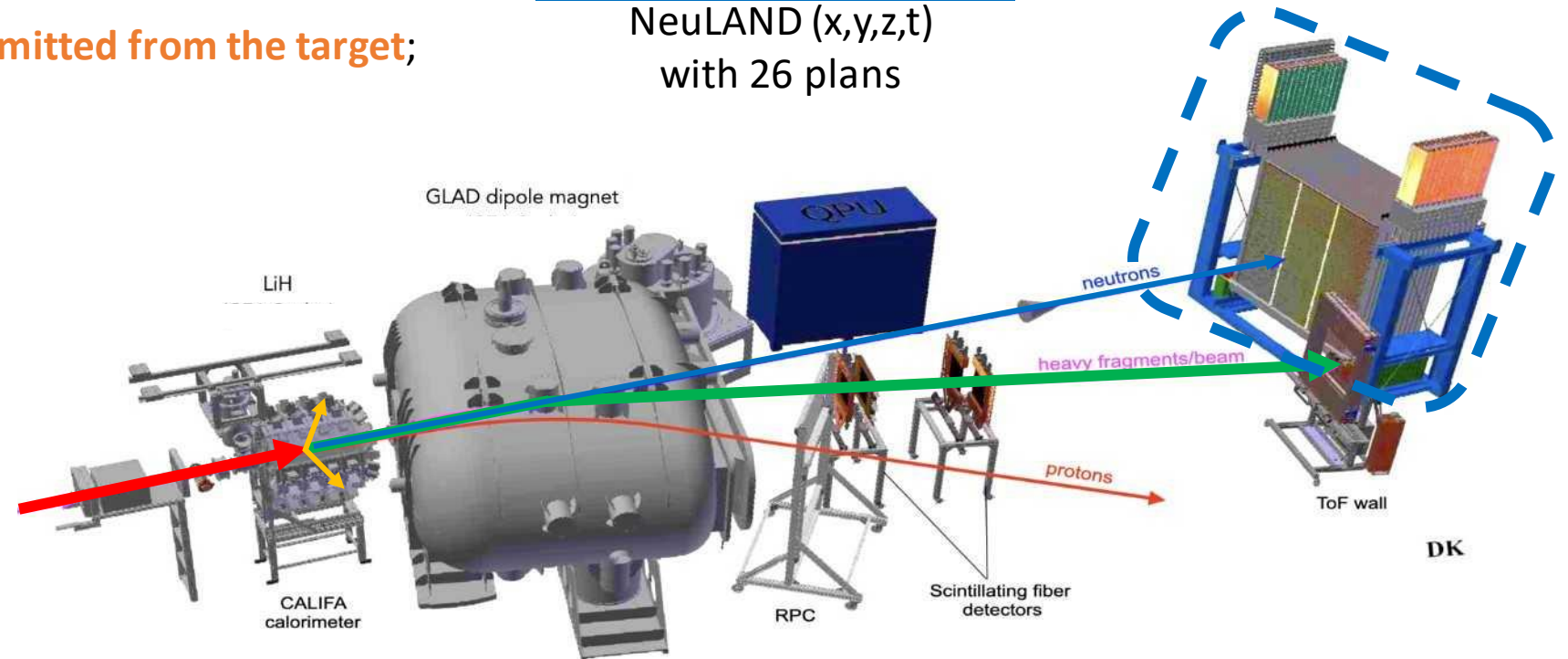
QFS reaction e.g.  $(p,pn)$  and  $(p,2p)$  in LiH

Complete measurement in inverse kinematics:

- **Incoming nucleus;**
- **Light particles and gammas emitted from the target;**
- **Outgoing fragment;**
- **Neutrons.**

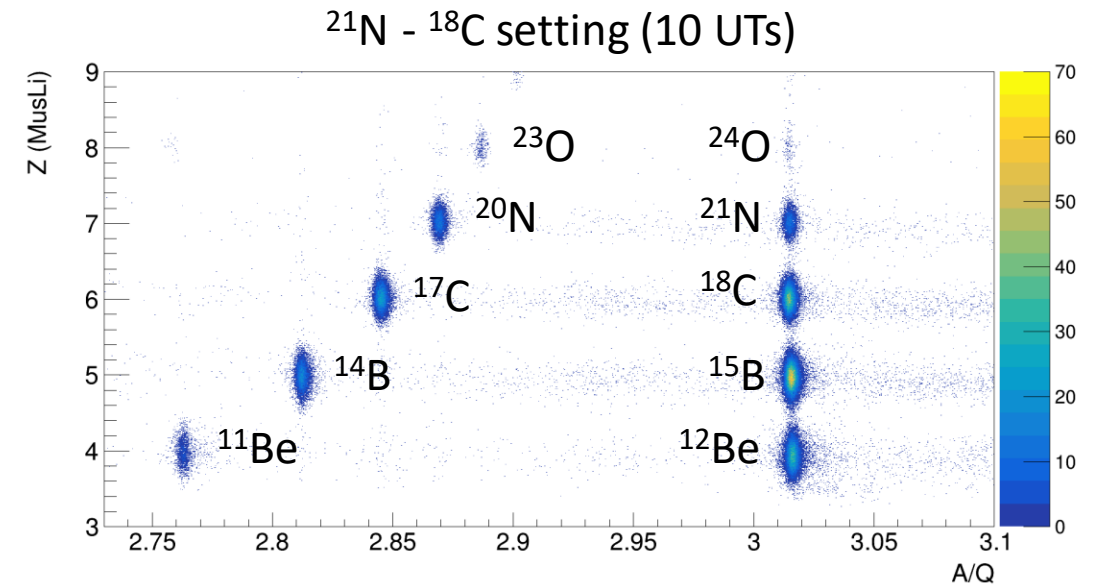
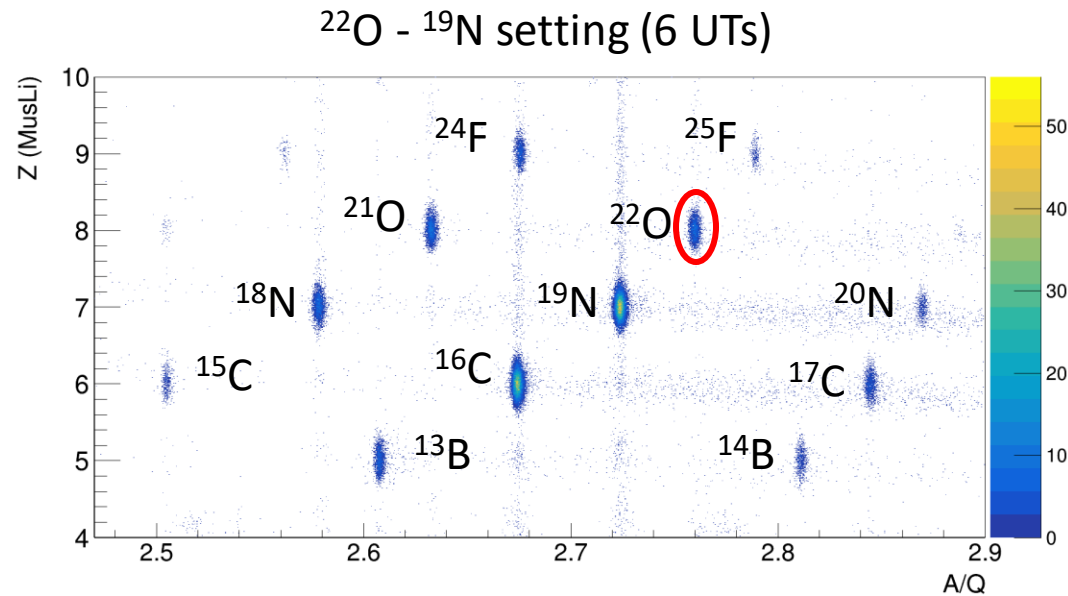


NeuLAND (x,y,z,t)  
with 26 plans



# Identification of the incoming nuclei

2 settings were used :

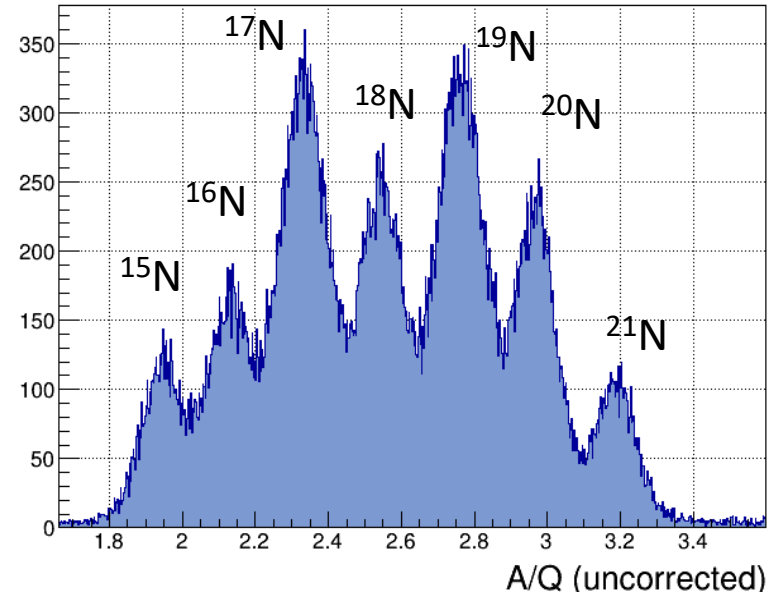
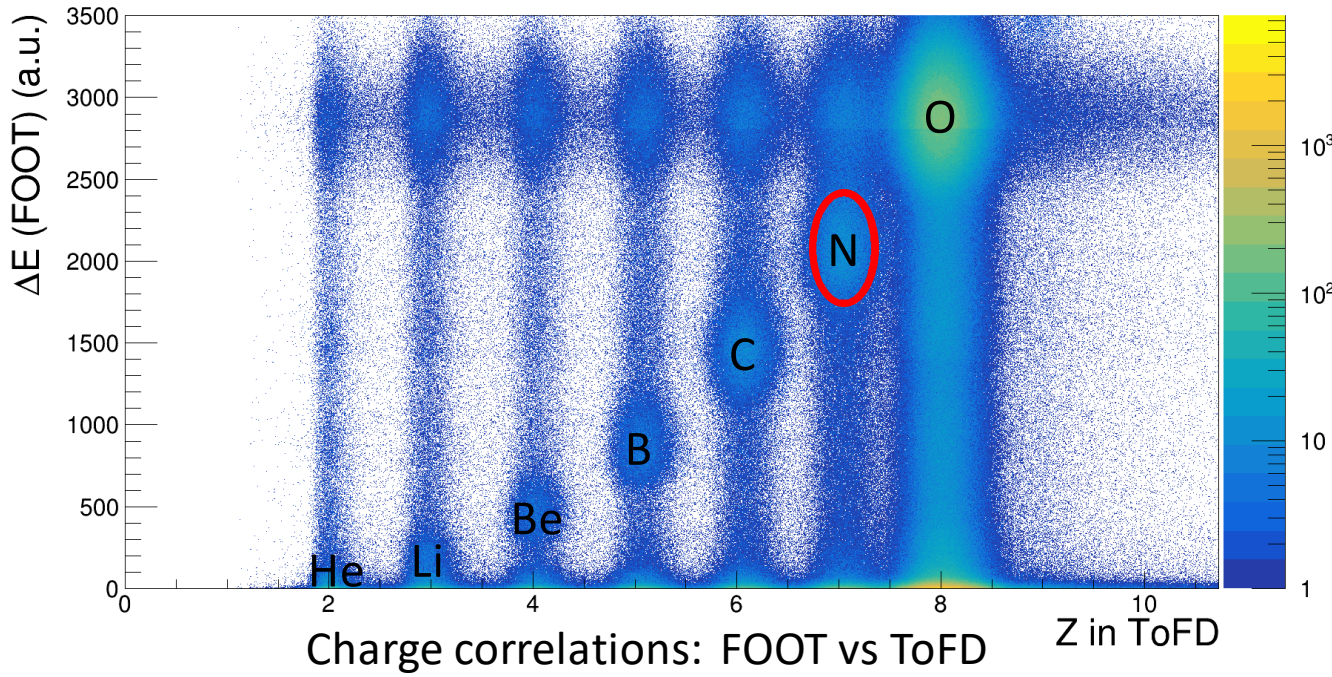


$\Delta E(\text{MusLi}) \rightarrow Z$   
(Bethe-Bloch)

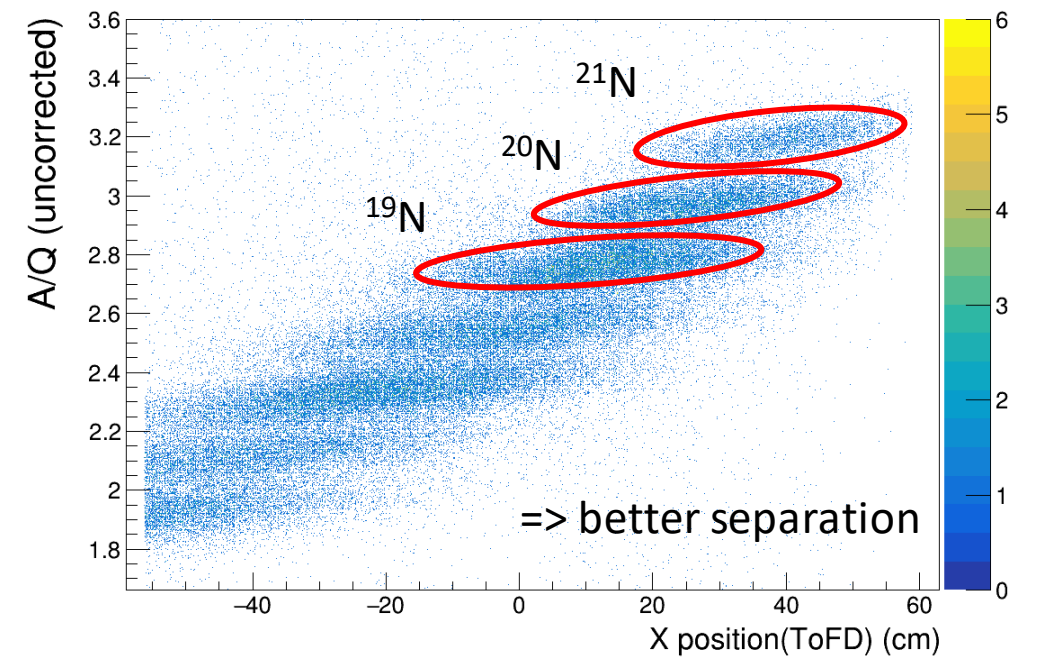
ToF (S2-LOS)  $\rightarrow \beta \cdot \gamma$

$$A/Q = \frac{B\rho_0 \cdot (1 - PosS2/D_{S2-CC})}{3.10716 \cdot \beta \cdot \gamma}$$

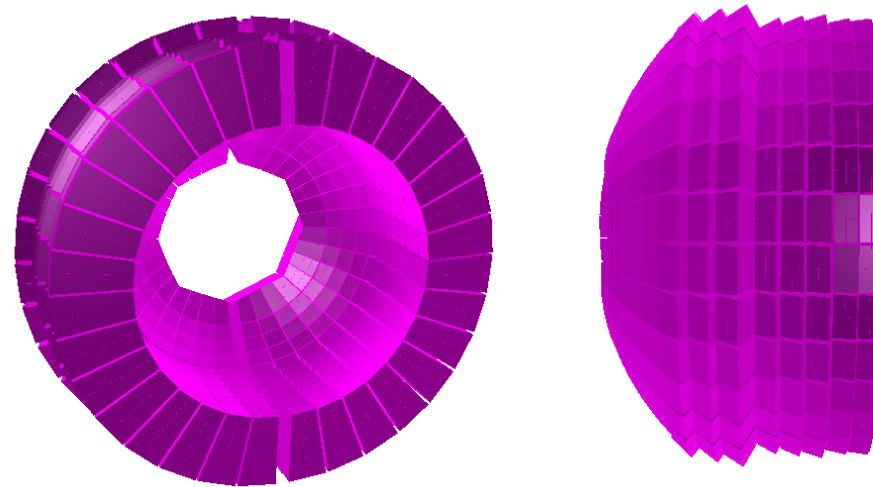
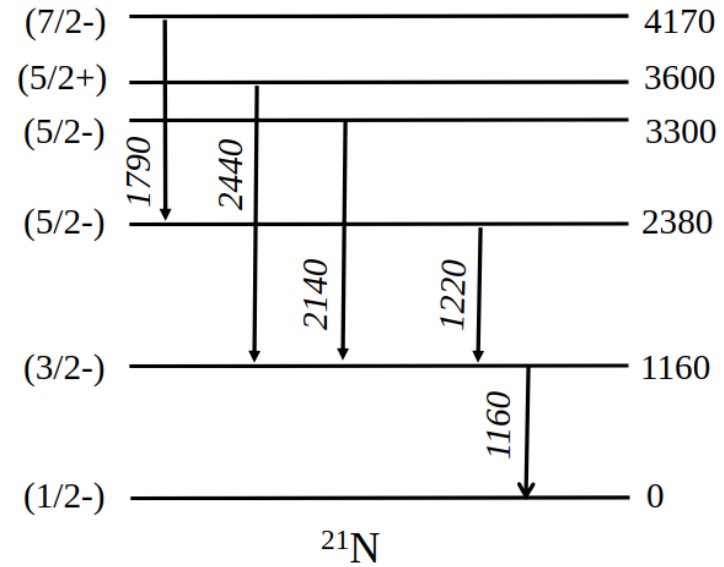
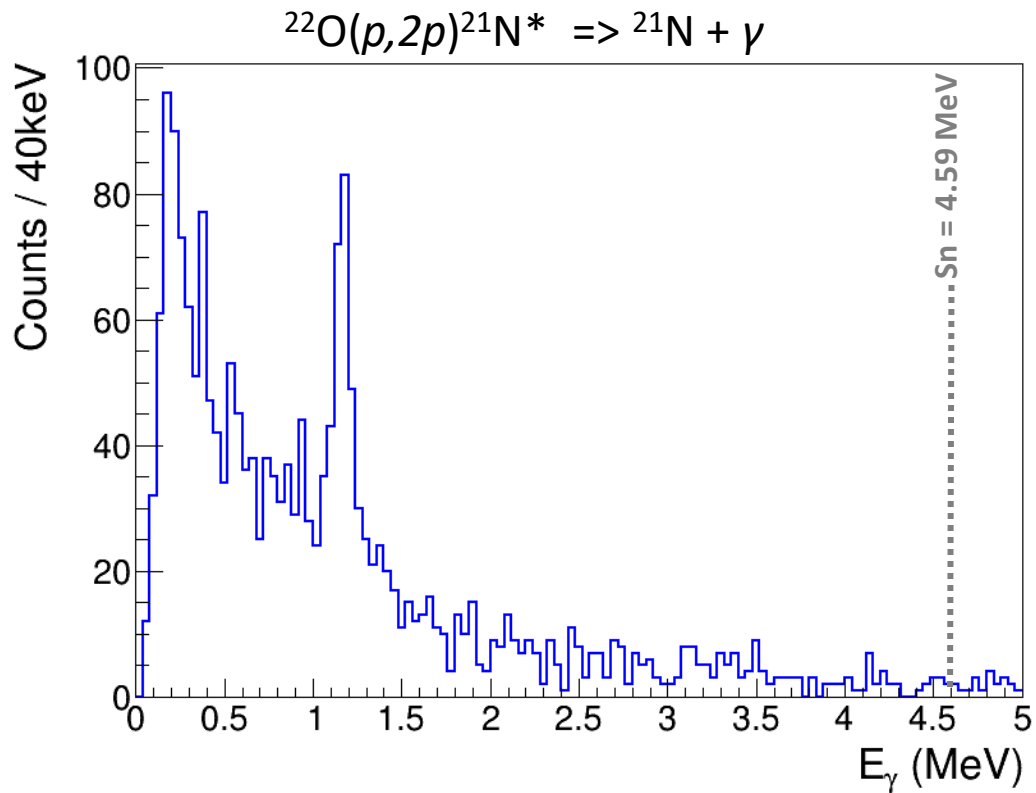
# Identification of the N isotopes from the $^{22}\text{O}(p,2p)^{21}\text{N}$ reaction



- Use of the energy losses in FOOTs and ToFD to reject events with a change of the Z in the air (reaction).
- To get the mass, a tracking algorithm allows to link positions before and after GLAD, with the propagation in the magnetic field (=> flight path).
- The inclusive cross section is then obtained by counting the  $^{21}\text{N}$  (bound states).

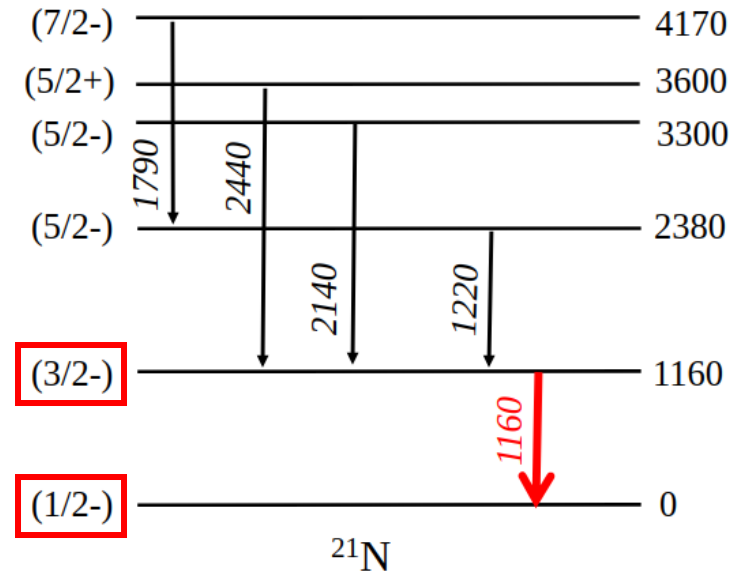
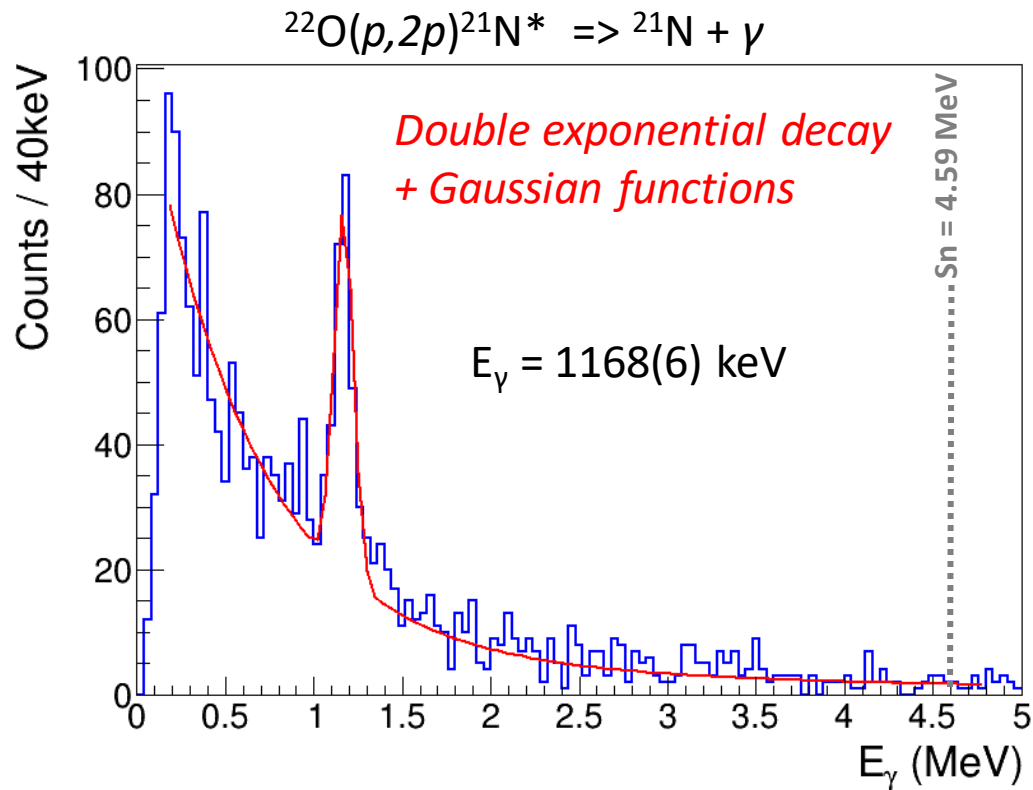


# Population of bound states in the $^{22}\text{O}(p,2p)^{21}\text{N}$ reaction



CALIFA (Barrel + Endcap): 1504 crystals, including 480 with 2 electronic gains (Endcap)

# Population of bound states in the $^{22}\text{O}(p,2p)^{21}\text{N}$ reaction



**Resolution:**

$\sigma = 40\text{keV}$  at  $E_\gamma = 1.170$  MeV

$\Rightarrow \text{FWHM} / E_\gamma = 8\%$

**Efficiency:**

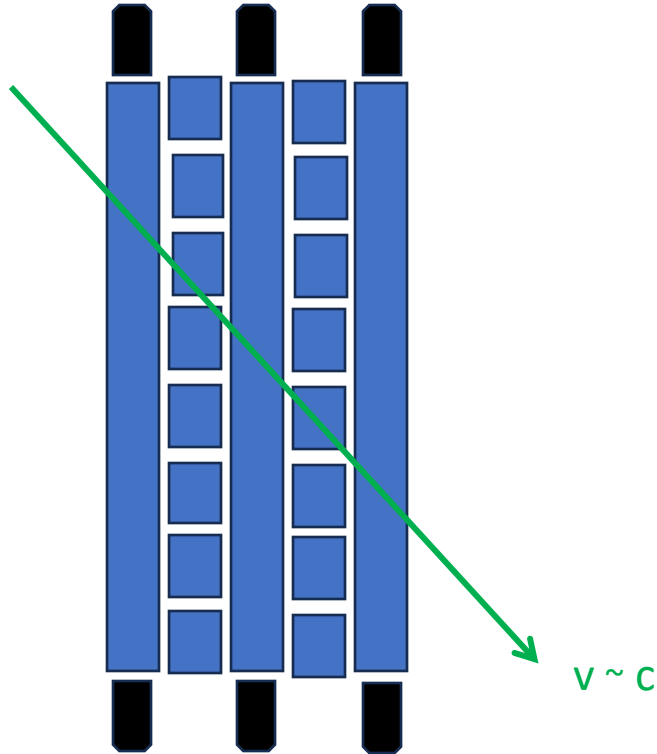
$\epsilon_\gamma(1.170\text{MeV}) = 26\%$

**Results:** 
$$\frac{N(3/2_1^-)}{N(1/2_{GS}^-)} = \frac{N(3/2_1^-)}{N_{incl} - N(3/2_1^-)} = 19.0(31)\%$$

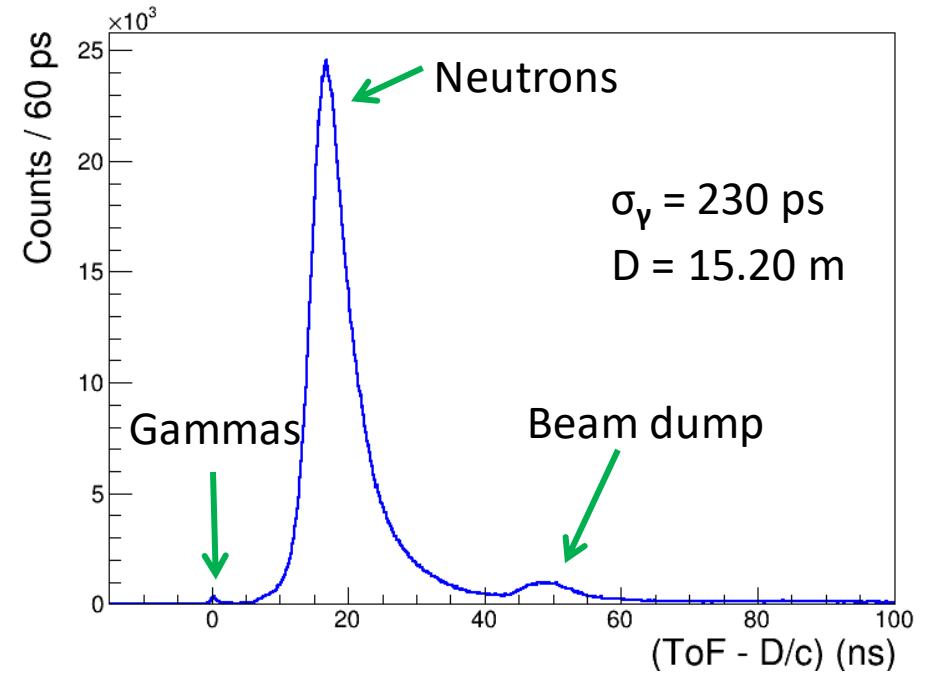
$\Rightarrow$  Among the bound states, the  $1/2_{GS}^-$  is the most populated by the  $(p,2p)$  reaction.

# NeuLAND and the invariant mass method

Alignment of the time difference of the two PMTs for each bar, using cosmic rays (muons) and a tracking algorithm.



Portion of NeuLAND crossed by a cosmic ray particle.

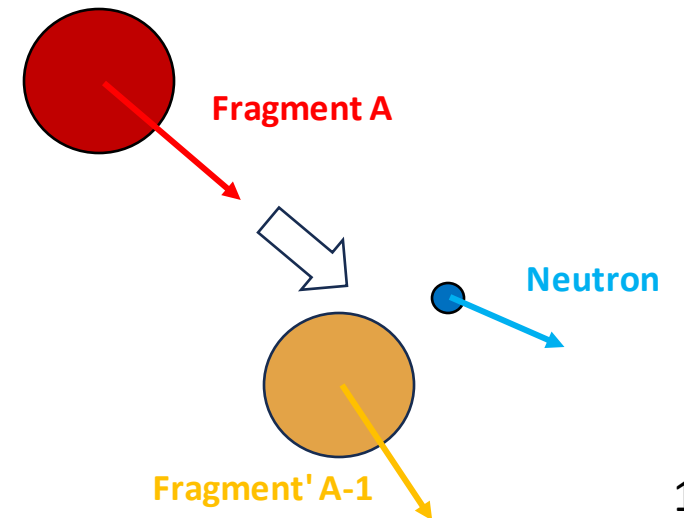


Use of the invariant mass method:

$$M_{inv} = \sqrt{\left(\sum_{i=0}^N E_i\right)^2 - \left(\sum_{i=0}^N p_i\right)^2}$$

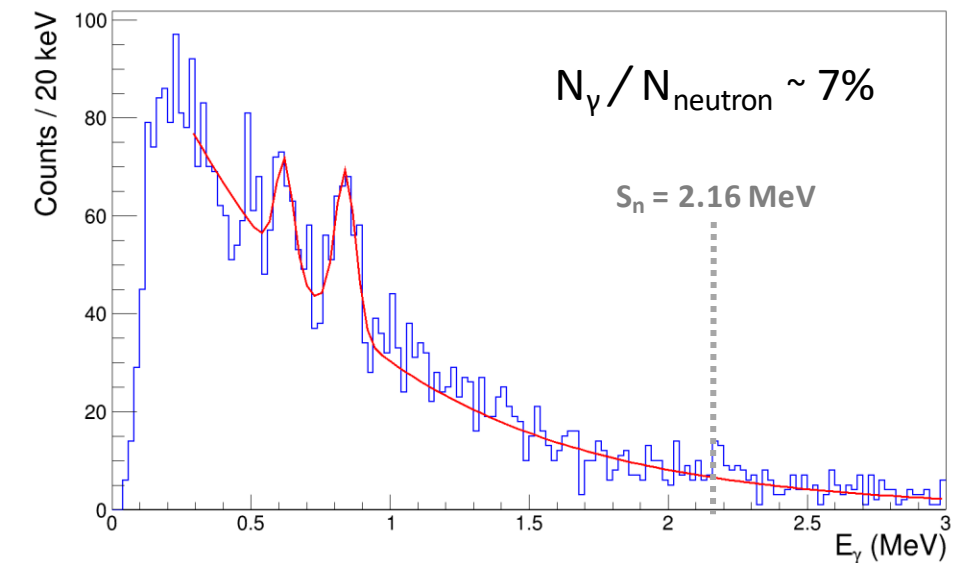
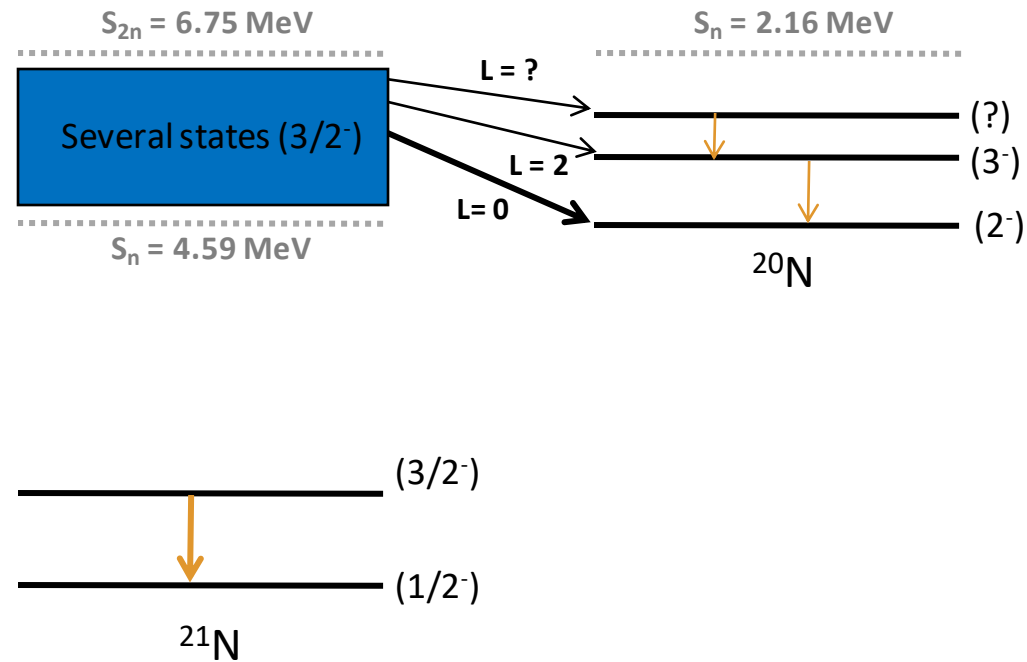
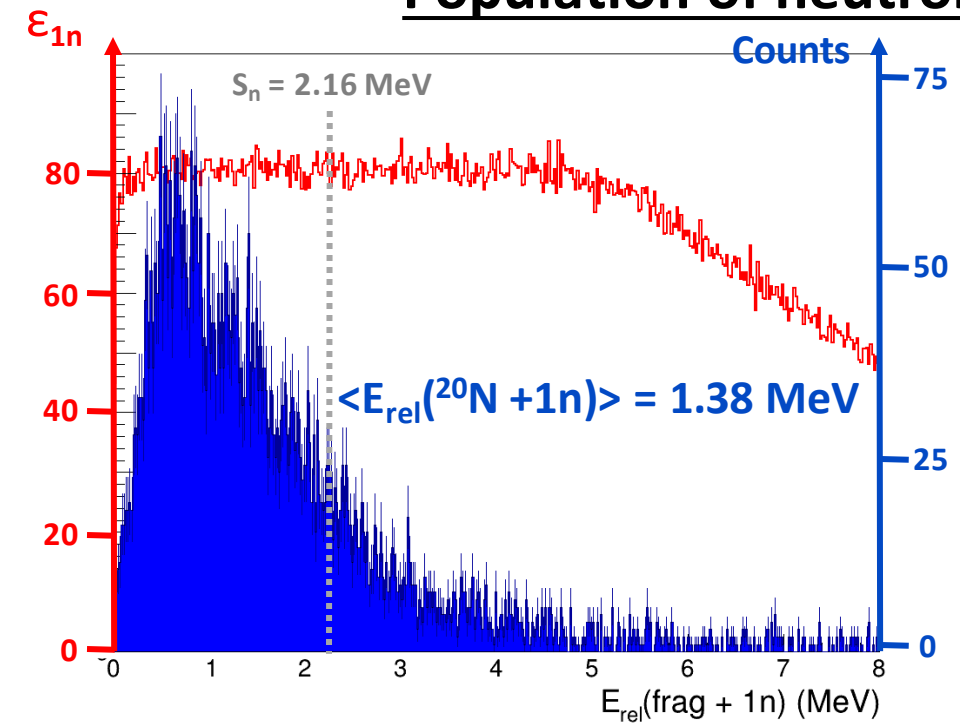
with the energy and momentum of the fragment and neutron(s)

$$E_{rel} = M_{inv} - \sum_{i=0}^N m_i$$





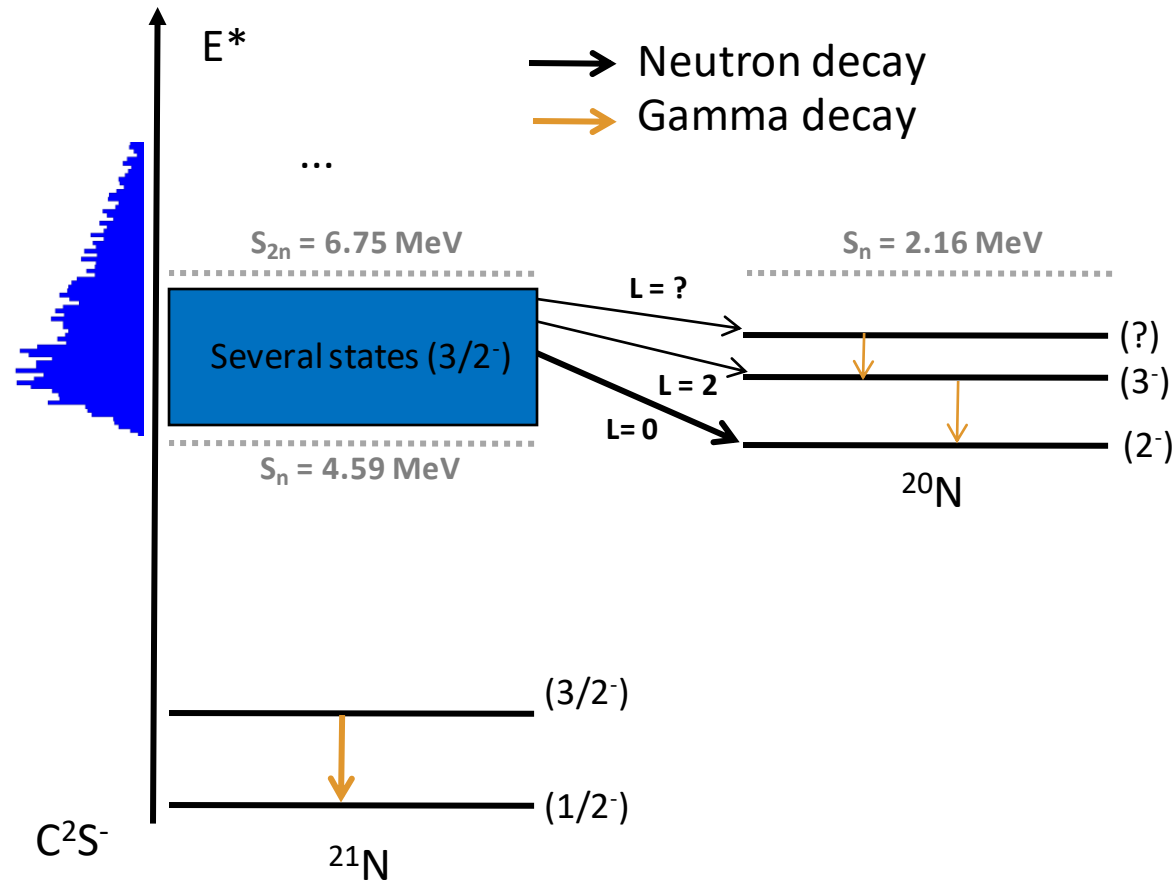
# Population of neutron unbound states in the $^{22}\text{O}(p,2p)^{21}\text{N}$ reaction



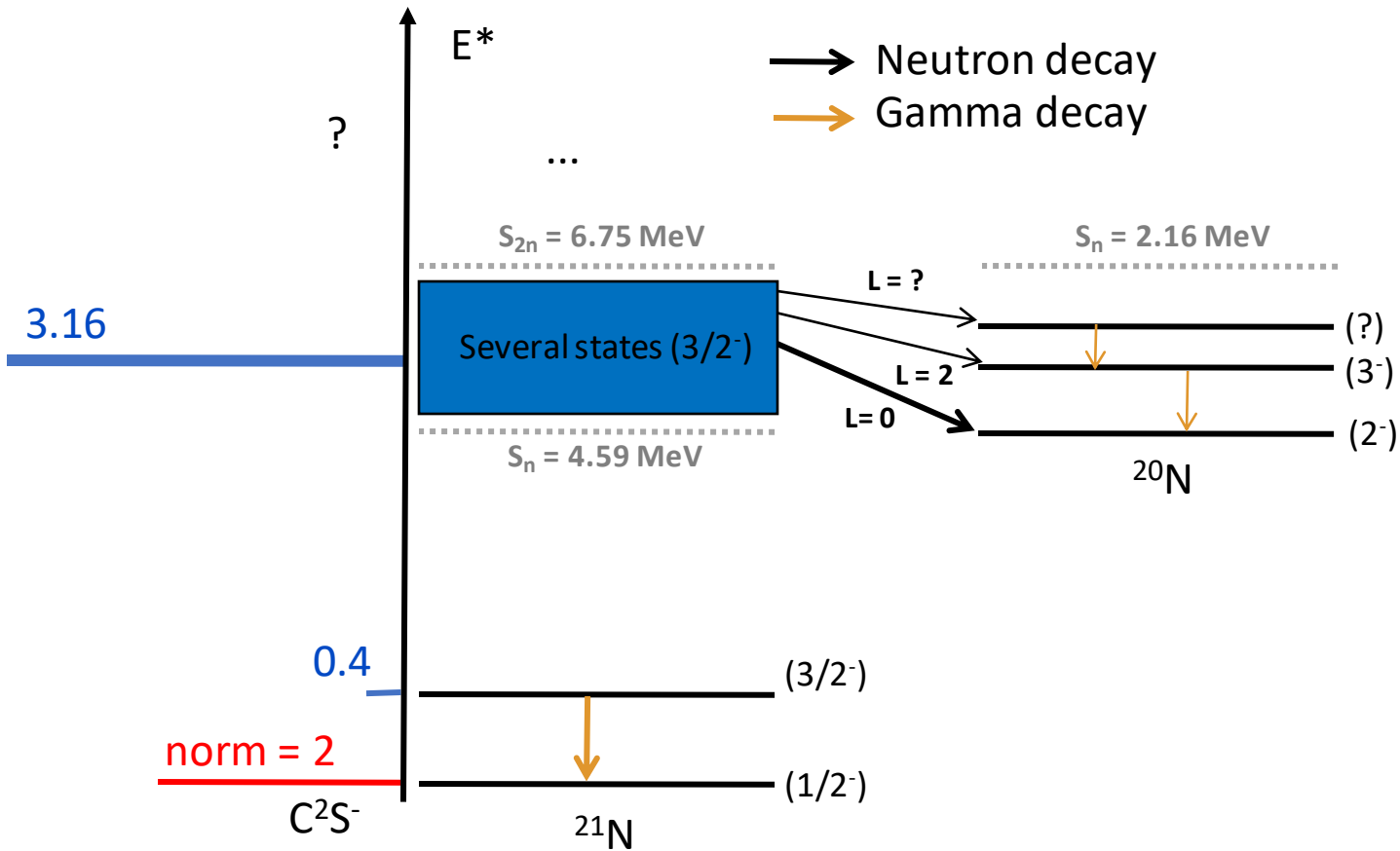
Fit of the  $E_{\text{rel}}$  distribution requires to take into account:

- Time resolution of NeuLAND --> already done;
- Effective resolution of the beta(fragment) --> straggling + detector resolution --> still ongoing.

# Conclusions and perspectives



# Conclusions and perspectives

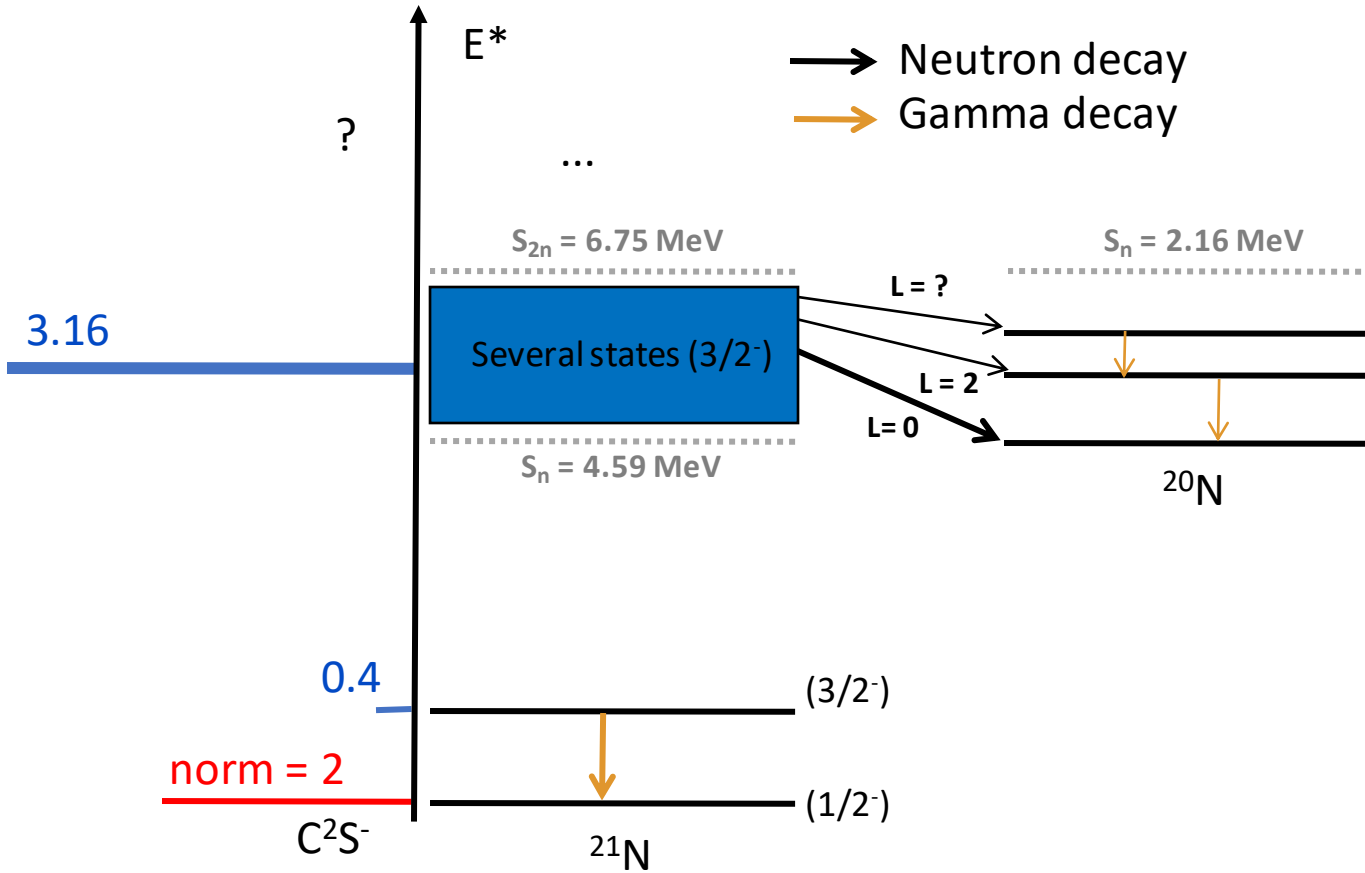


**Fraction of the strength recovered:**

$$\frac{N_{tot}(3/2^-)}{N(1/2_{GS}^-)} \geq \frac{N(3/2_1^-) + N_{1n}}{N_{incl} - N(3/2_1^-)} = 1.77(13)$$

A small fraction may be located above the  $S_{2n}$

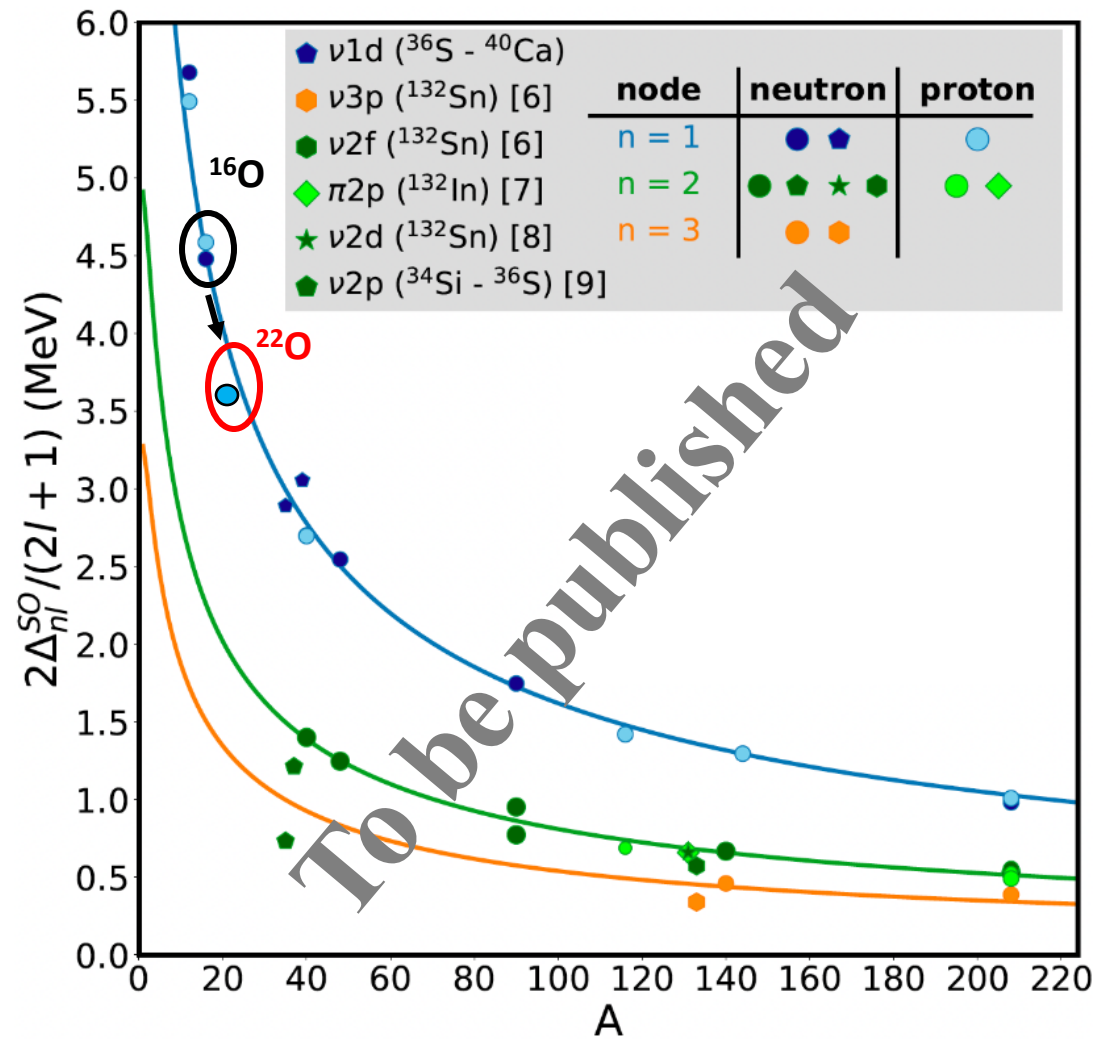
# Conclusions and perspectives



First estimation of the proton gap in  $^{22}\text{O}$ :

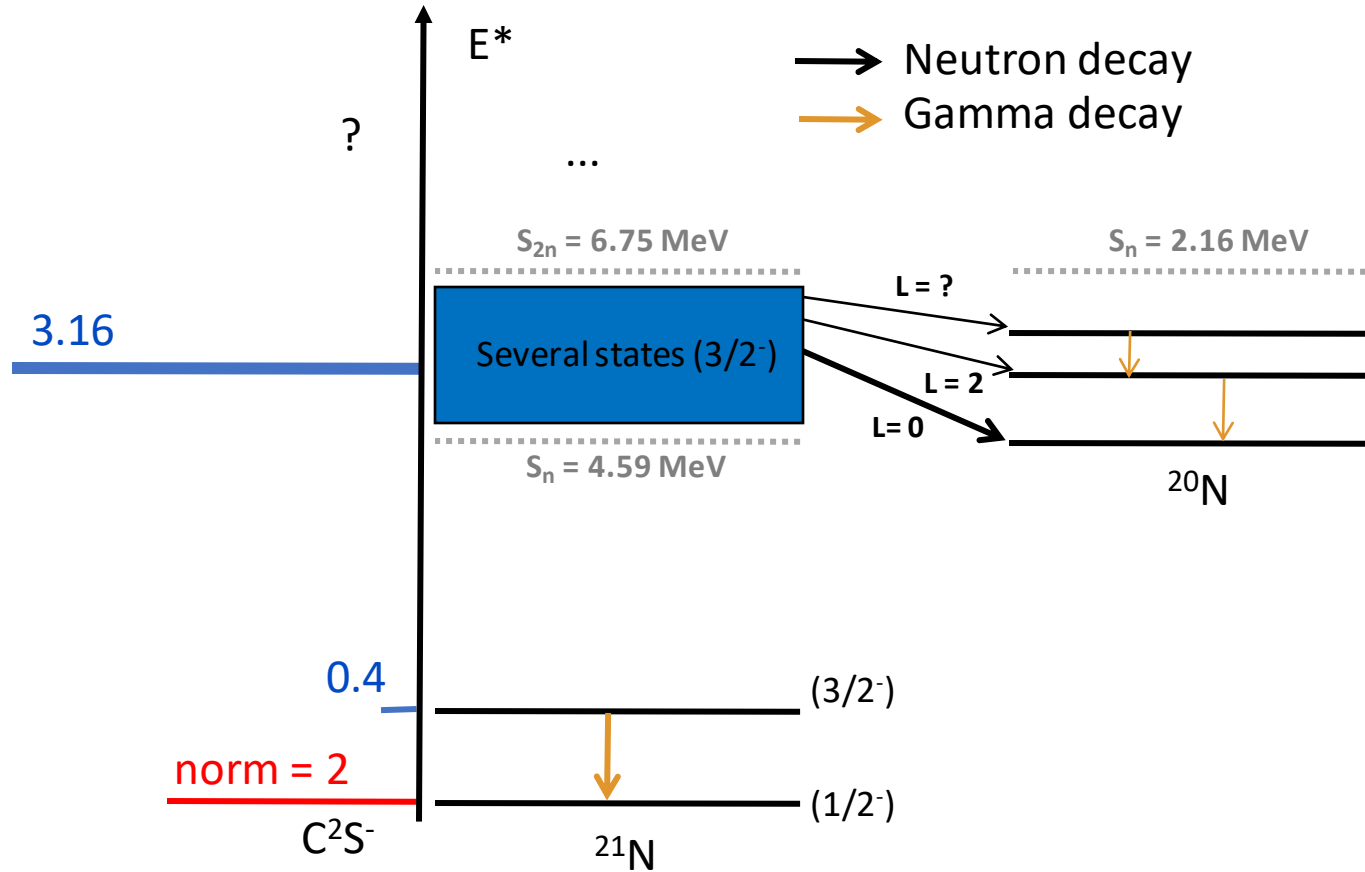
$$\langle 0p_{3/2} \rangle_{s.p.} \geq \frac{E^*(3/2_1^-)N(3/2_1^-) + N_{1n}E_{1n}^*}{N(3/2_1^-) + N_{1n}}$$

$$\langle 0p_{3/2} \rangle_{s.p.} - \langle 0p_{1/2} \rangle_{s.p.} \geq 5.46 \text{ MeV}$$



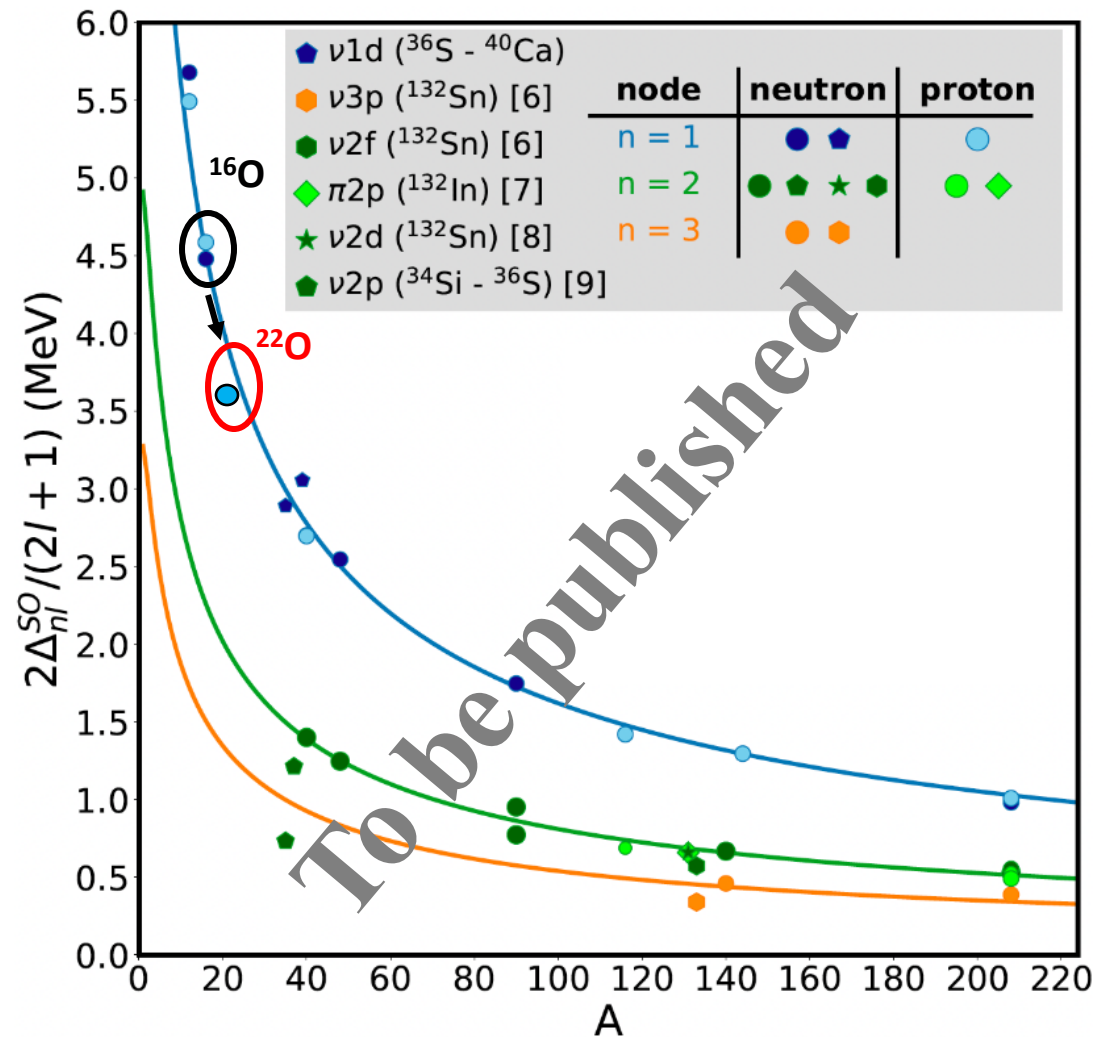
➡ Deviation from the Mairle's trend about 350 keV

# Conclusions and perspectives



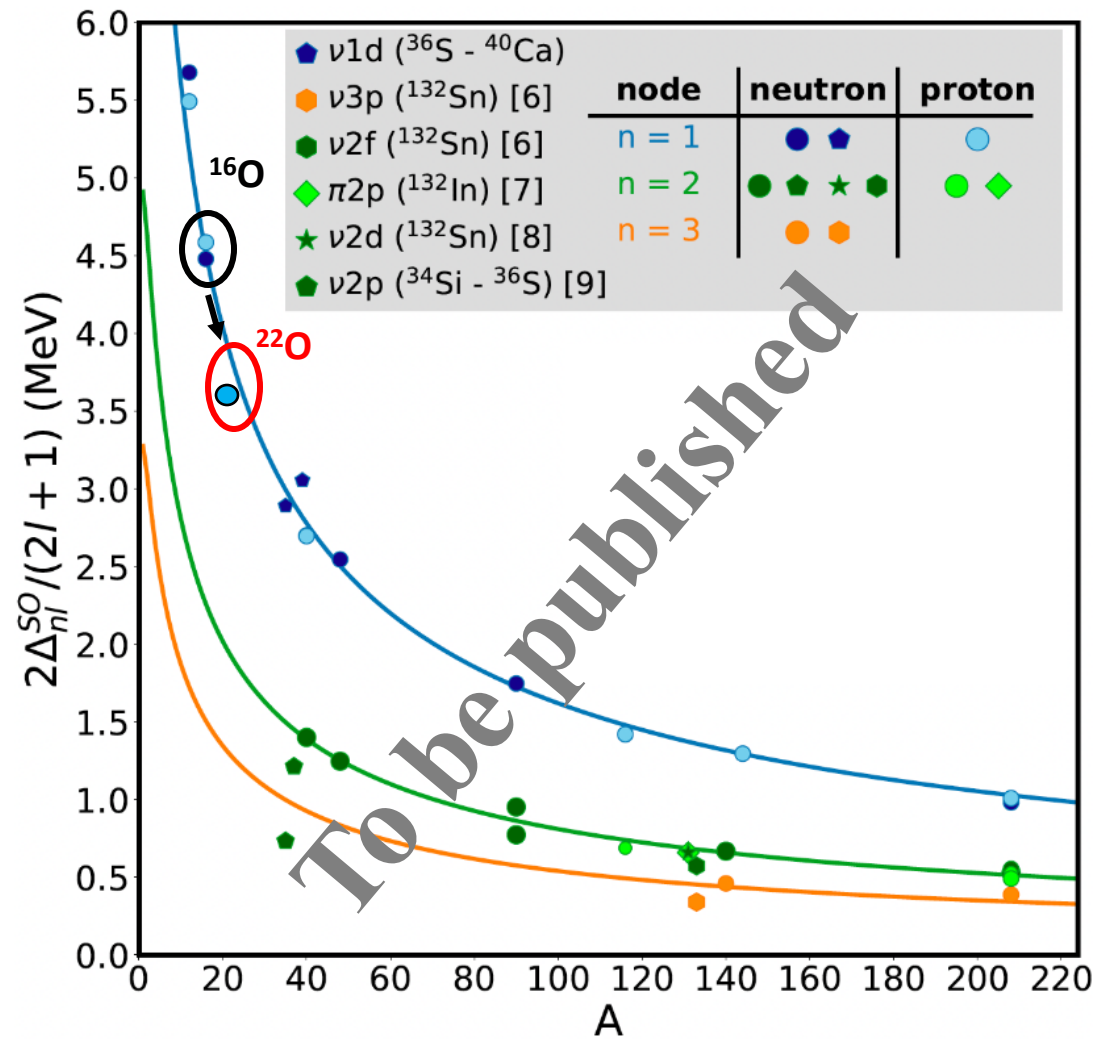
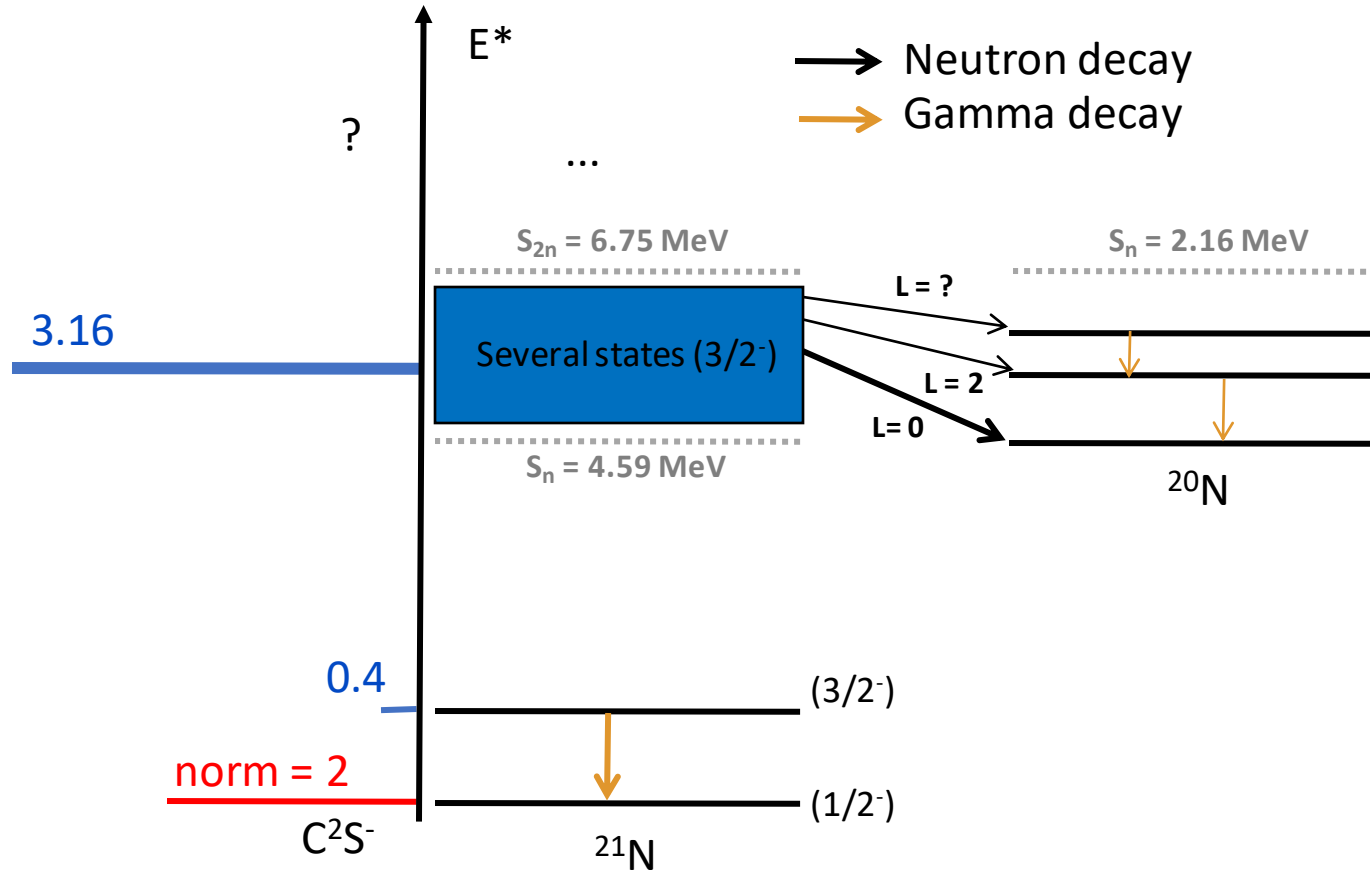
## Perspectives :

- Study of the  $^{21}\text{O}$  momentum via  $^{22}\text{O}(p,pn)$  (6 neutrons in the neutron orbital  $0d_{5/2}$  ?);
- 1n spectroscopy, w. gamma-neutron coincidences;
- Analysis of unbound states decaying by 2n emission.



➡ Deviation from the Mairle's trend about 350 keV

# Conclusions and perspectives

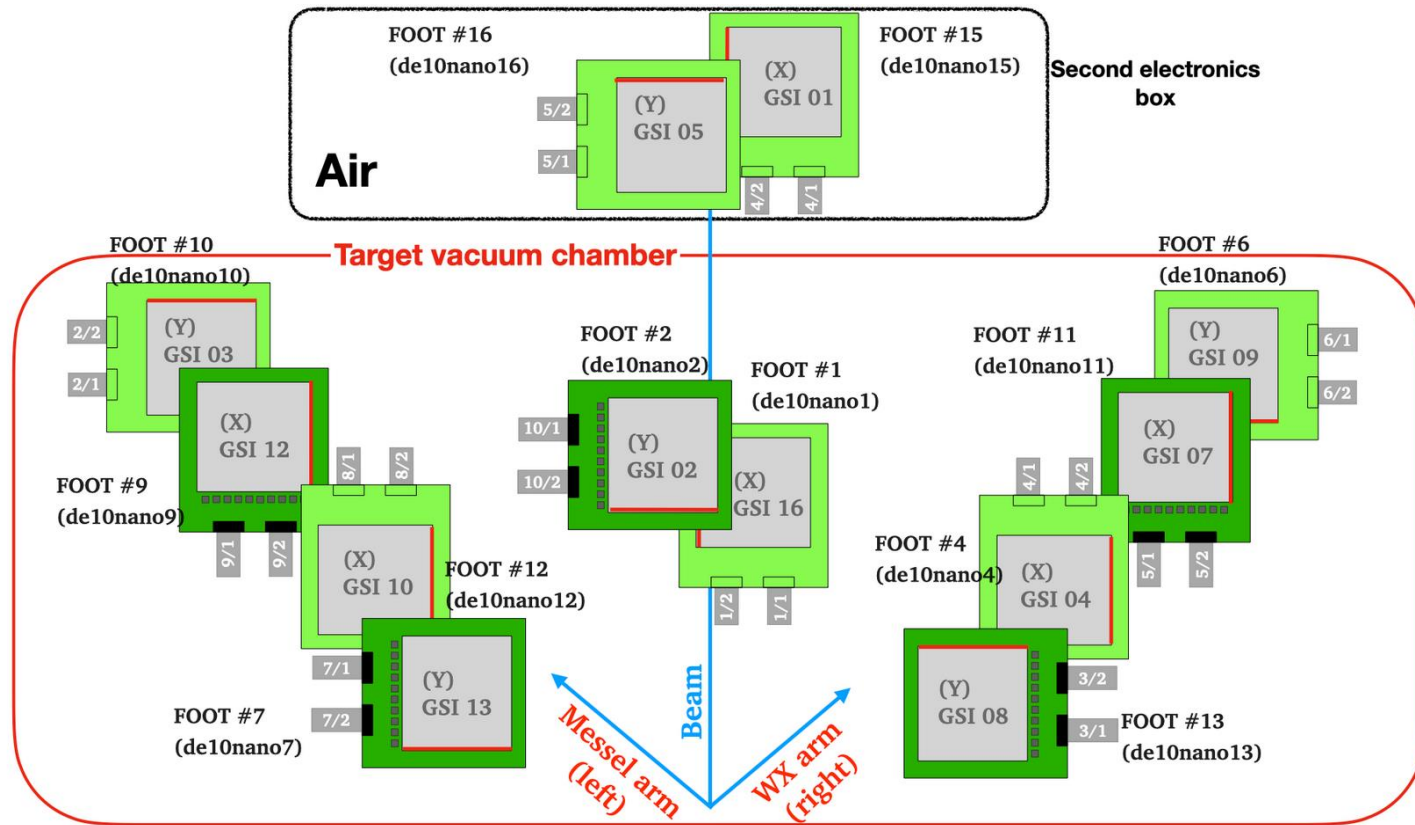


**Thank you  
for your attention !**

➡ Deviation from the Mairle's trend about 350 keV

# Backup Slides

# Tracking around the target



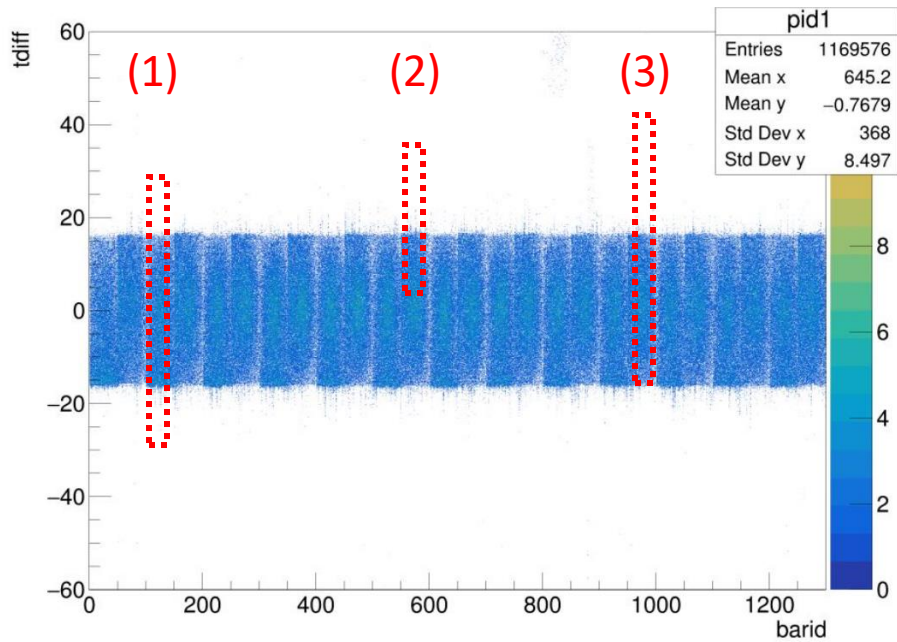
FOOTs mapping : 4 on each side + 4 in-beam



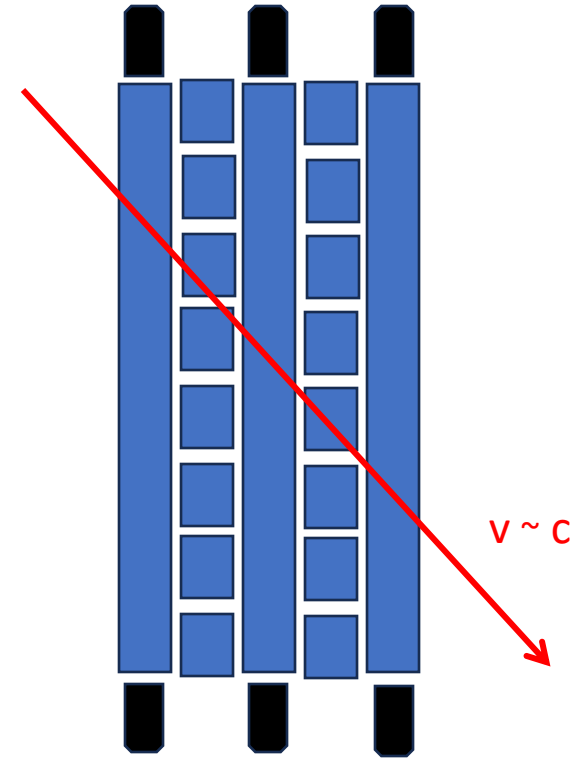
# NeuLAND calibration

PMTs time for one bar -> position within the bar + ToF (target-bar)

1) Alignment of the time difference of the two PMTs for each bar, using cosmic rays and a tracking algorithm



Time difference left/right or bottom-top PMTs vs Bar Id, for on-spill events



Portion of NeuLAND crossed by a cosmic ray particle.

For each bar, we can define:

Time diff :  $T1 - T2$   
-> Effective speed of light

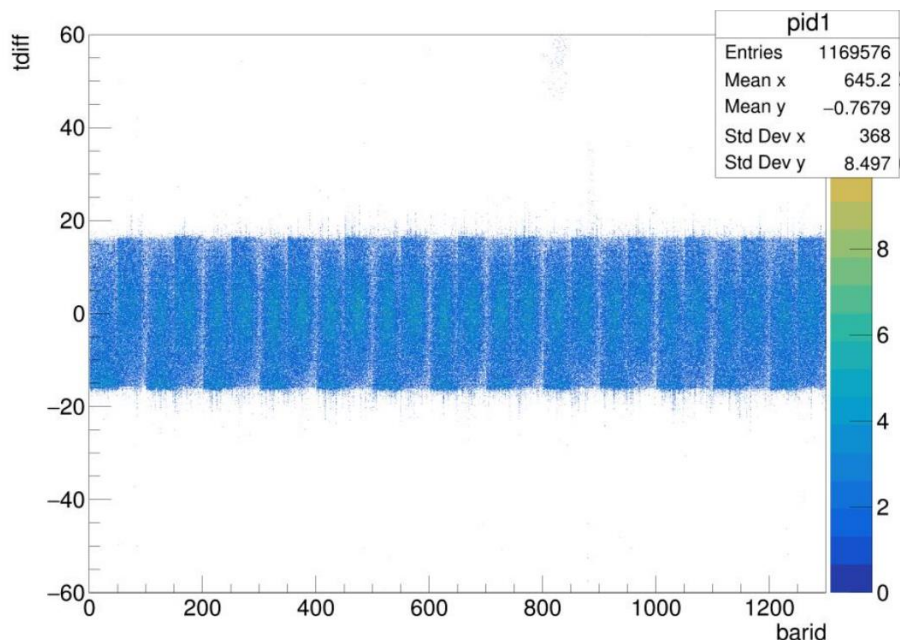
Time synch :  $T1 + T2$   
-> Global offset

- (1) => diff correction
- (2) => synch correction
- (3) => both of them

# NeuLAND calibration

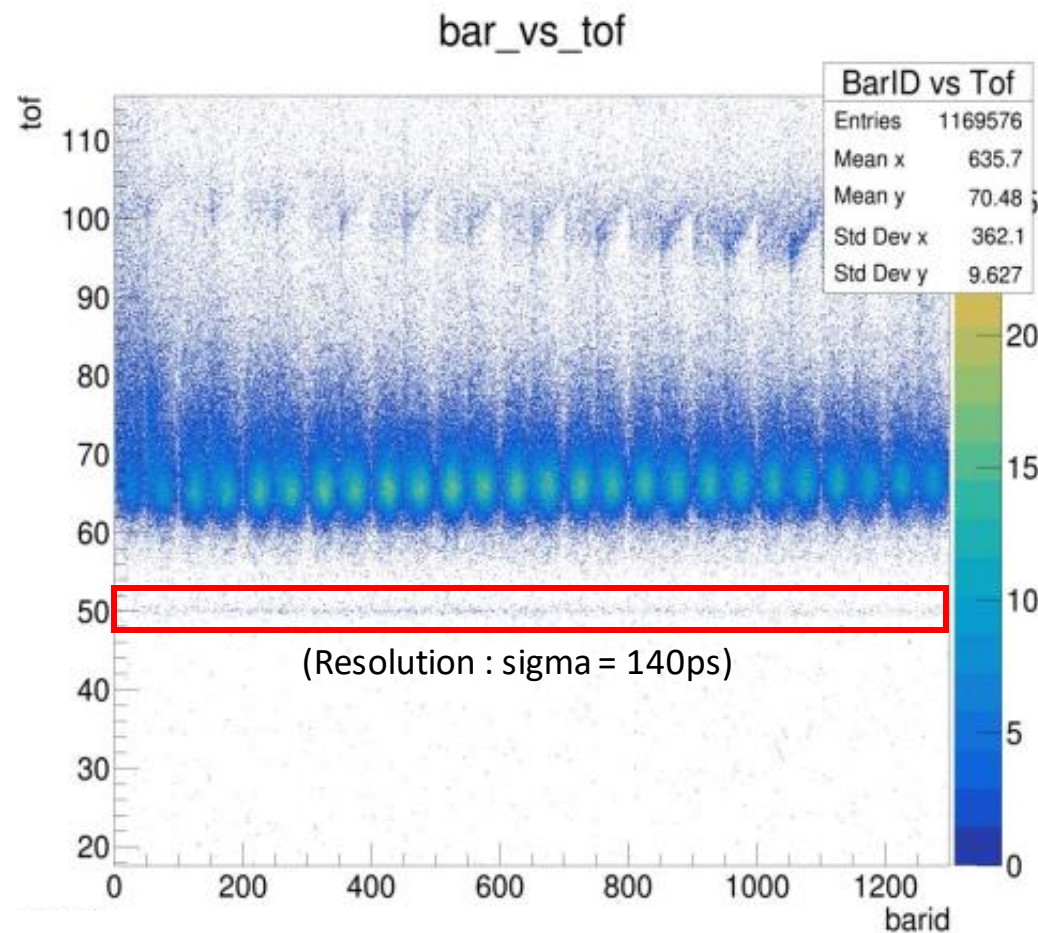
PMTs time for one bar -> position within the bar + ToF (target-bar)

- 1) Alignment of the time difference of the two PMTs for each bar, using cosmic rays and a tracking algorithm



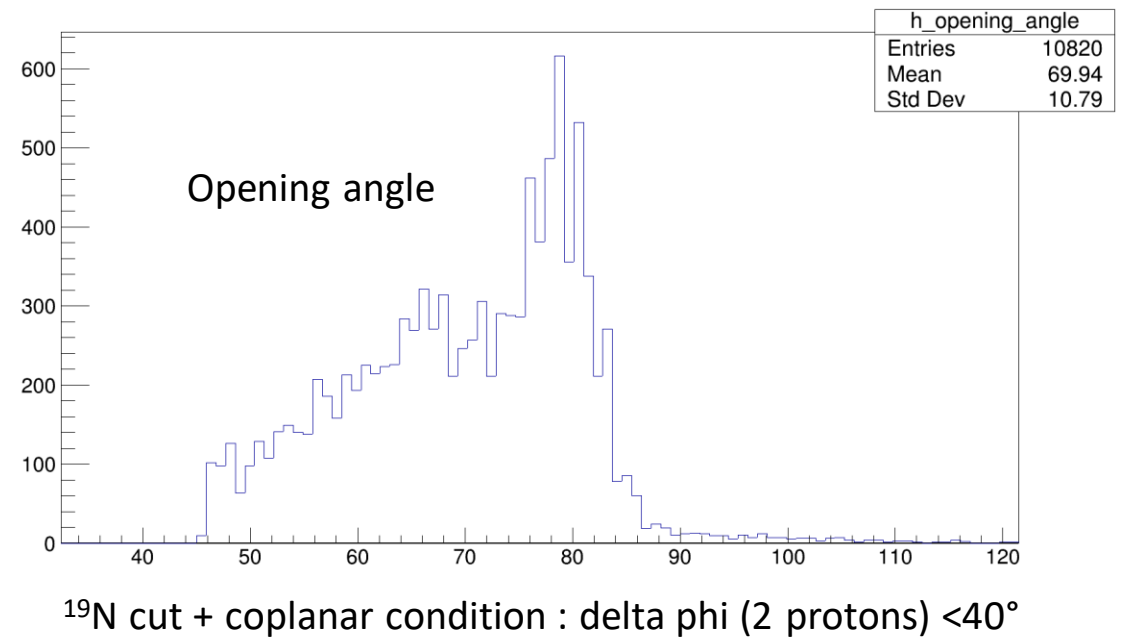
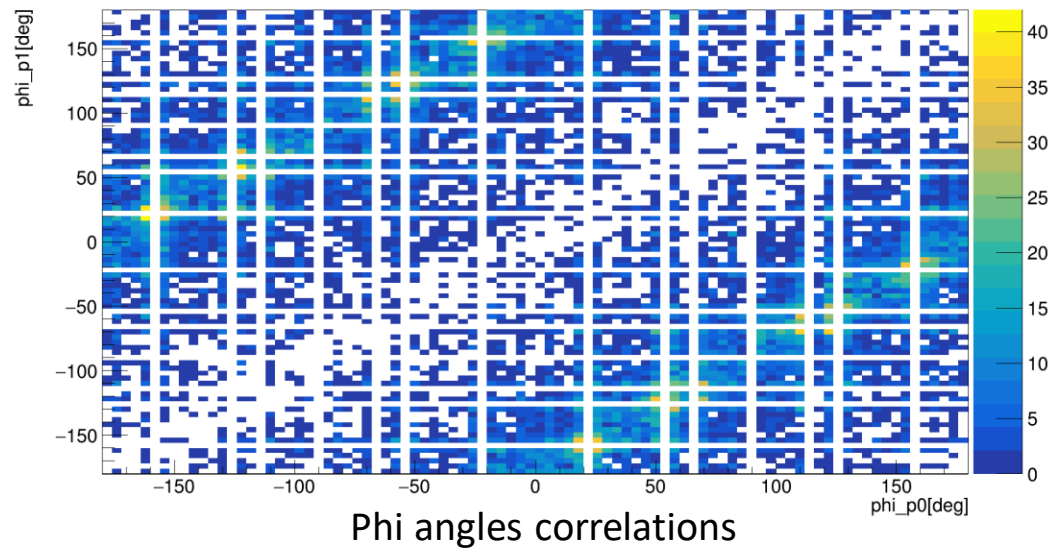
Time difference left/right or bottom-top PMTs vs Bar Id, for on-spill events

- 2) Fine tuning with the gamma peak

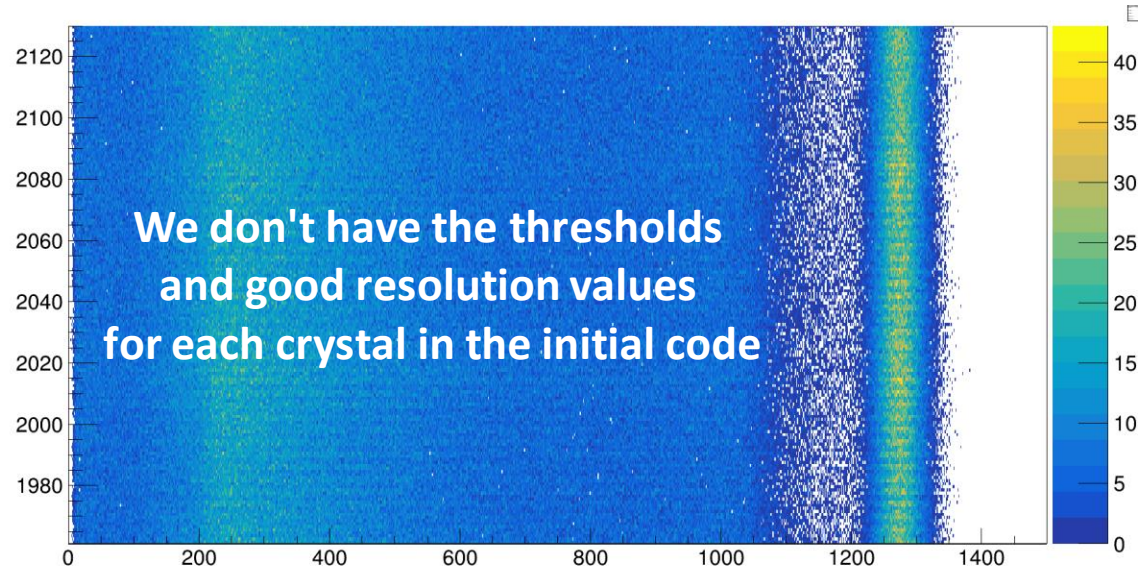


ToF (NeuLAND Bar – LOS) vs Bar Id for on-spill events

# Califa and the QFS reactions

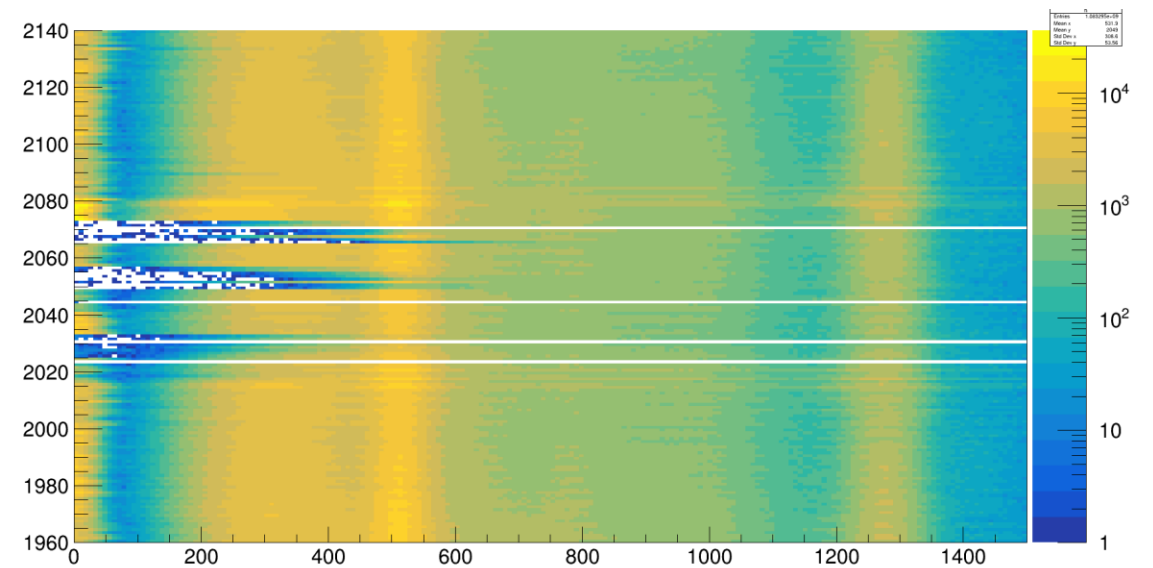


# Modifications of the gamma simulations

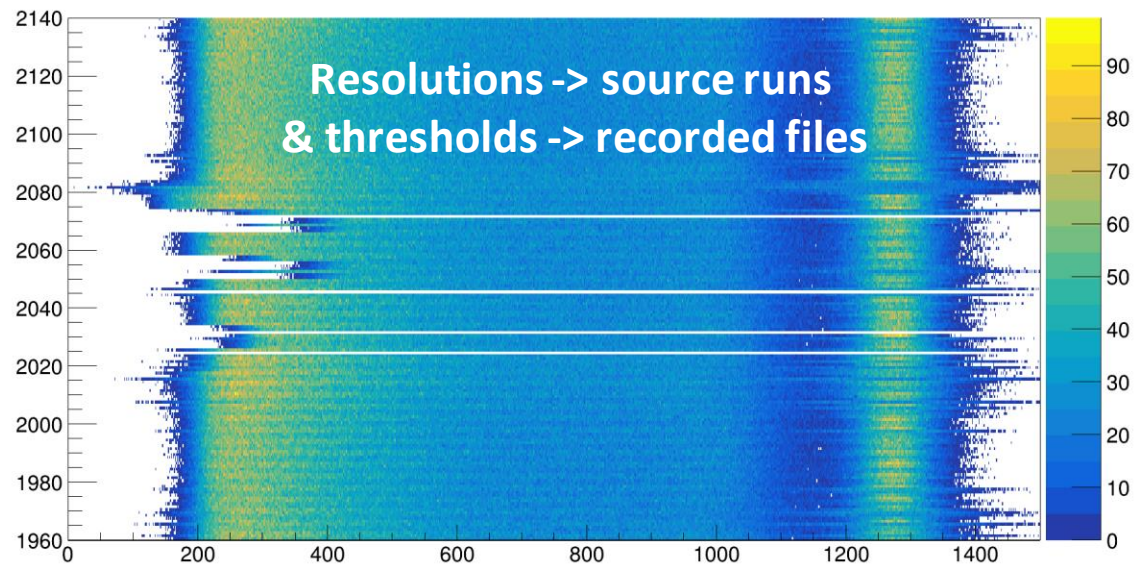


We don't have the thresholds  
and good resolution values  
for each crystal in the initial code

Crystal Id vs energy (simulation): 1274keV peak



Crystal Id vs energy ( $^{22}\text{Na}$  source)



Resolutions -> source runs  
& thresholds -> recorded files

Crystal Id vs energy (simulation): 1274keV peak

Use of simulations in gamma analysis:

-> To get the energy of the transitions

-> To obtain the associated cross section